DIC Challenge - Summary of Results

E. M. C. Jones
University of Illinois

November 11, 2014

Version 1

1 Copyright

The author requests that users of this code notify the author of any modifications, improvements, or adaptations they make to this code, so that such modifications can be addressed and possibly incorporated in future versions of this code.

Contact information:
Elizabeth Jones
Beckman Graduate Fellow
NSF Graduate Research Fellow
Ph.D. Candidate in Theoretical and Applied Mechanics
University of Illinois at Urbana-Champaign
ElizabethMCJones@gmail.com
www.linkedin.com/in/elizabethmcjones/

2   Acknowledgments

3   Introduction

This document provides a complete evaluation of the digital image correlation (DIC) code, Improved Digital Image Correlation (DIC), submitted to Matlab Central File Exchange by Elizabeth Jones (Fild ID #43073). For documentation on the function and usage of the code itself, the reader is referred to the accompanying PDF document "Matlab based DIC code documentation."

The precision and accuracy of the code was evaluated using standard test images provided by the Society for Experimental Mechanics (SEM) DIC Challenge. The complete image sets are available from the DIC Challenge website. In total, 13 image sets covering different aspects of the performance of the code were evaluated: rigid translation (image sets 1-7), rigid rotation (image sets 8-9), large strain (image set 10), constant strain and strain discontinuity (image set 11b), sinusoidal variation of the strain (image set 14) and overlapping strain peaks (image set 15). The deformations depicted in image sets 1-11, 14, and 15 were generated with different computer algorithms. The author assumes that the errors resulting from the image transformations are negligible compared to the errors resulting from the correlation process. No analytic solution was provided for image set 10; therefore, only a qualitative evaluation of this image set is performed. Image set 12 is an experimental image set with no known solution; a discussion of the performance of the code for this image set is provided in the main documentation for the code, "Matlab based DIC code documentation." Image set 14 is another experimental image set with no known solution; it was not evaluated.

The follow parameters are used for all the analyses presented in this document unless otherwise noted: step size of 5 pixels, threshold value of 0.5 for the minimum correlation coefficient, search zone of 2, Gaussian distribution of the weighting factors during the smoothing of displacements, displacement interpolation over 16 node, bi-cubic finite elements for strain calculations, and finite strain values (i.e. E_{xx}) rather than infinitesimal strain values (i.e. e_{xx}). Throughout this document, the smoothing parameters are listed as [smoothing kernel size, number of smoothing passes]. The smoothing parameters refer to the smoothing of the displacements prior to calculating strains. No post-processing of the strains is performed.

For simplicity and clarity, only one displacement (horizontal, U, or vertical, V) and one normal strain (horizontal, E_{xx}, or vertical, E_{yy}) are shown for the rigid body translations (image sets 1-5)and rigid body rotations (image sets 8-9). The other displacement and strain components follow similar trends with regard to smoothing parameters, subset size, threshold value, etc.

Strains calculated from unsmoothed displacements are extremely noisy and cannot be used. Therefore, only strains calculated from smoothed displacements are presented in the evaluations.

A concise summary and a complete summary of the results are found in Sec. 4. Detailed results for each image set are found in the following sections.

4   Results Summary

Table 1 provides a concise summary of the results of the evaluation of this DIC code using the images provided by the DIC Challenge. The noise threshold provides an approximate baseline for the noise or error associated with the code. Table 2 provides a summary of the results of each image set. Full explanations of the results for each image set are found in the following sections.

Table 1. Concise Summary of Correlation Results

Deformation		Samples	Noise Threshold* Displacement (pixels)	Noise Threshold* Strain (% strain)	Comments
Rigid Translation	Good speckle pattern	1, 3, 5, 6, 7	0.03	0.06	Quality of speckle pattern greatly influences noise threshold
	Poor speckle pattern	2, 4	0.07-0.17	0.20-0.63	
Rigid Rotation		8, 9	0.03	0.07	1 deg. applied rotation
			0.25	0.45	5 deg. applied rotation
Large Strain		10	--	--	Analytic solution unknown
Constant Strain		11	0.04	0.06	0.2 % applied strain — Error is approximately 30 % of constant strain value
			0.04	0.12	0.4 % applied strain
Strain Discontinuity		11	46	--	0.2 % applied strain — Width of strain discontinuity
			61	--	0.4 % applied strain
Sinusoidal Strain Modulations		14	0.03	0.10	$1.8*10^{-3}$ pixels^{-1} average applied strain frequency
			0.06	0.36	$8.8*10-3$ pixels-1 average applied strain frequency
Overlapping Strain Peaks		15	--	1.3	Ratio of peak spacing to peak width of 1.2 — Error is approximately 24 % of maximum strain value (5.4 % strain)
				2.6	Ratio of peak spacing to peak width of 0.2 — Error is approximately 30 % of maximum strain value (8.8 % strain)

* The noise threshold is taken as 3*(standard deviation) of the error.

3

Table 2. Complete Summary of Correlation Results (part 1)

Sample No.	Deformation	Speckle Pattern
1	Rigid translation; 0.05 pixel increments up to 1.00 pixel	Good speckle pattern; varying contrast
2	Rigid translation; 0.05 pixel increments up to 1.00 pixel	Poor speckle pattern; low contrast
3	Rigid translation; 0.1 pixel increments up to 1.00 pixel	Good speckle pattern
4	Rigid translation; 0.1 pixel increments up to 1.00 pixel	Poor speckle pattern; low contrast
5	Rigid translation; 0.1 pixel increments up to 1.00 pixel	Good speckle pattern; varying contrast
8	Rigid rotation; 1 deg increments up to 9 deg	Good speckle pattern
9	Rigid rotation; 1 deg increments up to 9 deg	Good speckle pattern
11	Constant positive strain on left half of image, constant negative strain on right half of image, strain discontinuity in center of image	Good speckle pattern
14	Sinusoidal variation in strain with increasing frequency and amplitude	Good speckle pattern; varying contrast across individual images
15	Modulating strain with increasing distance between strain peaks	Good speckle pattern

Table 1. Complete Summary of Correlation Results (part 2)

Displacement (pixels)		Strain (% strain)		Comments	
Error	**Std. Dev.**	**Error**	**Std. Dev.**	**Comments**	
0.007	0.004	0.017	0.014	Subset 20, Smooth 11,3; Averaged over all images	
0.050	0.039	0.187	0.146	Subset 30, Smooth 11,3, Thresh 0.5; Averaged over all images	
0.005	0.004	0.015	0.013	Subset 20, Smooth 11,3; Averaged over all images	
0.023	0.014	0.058	0.045	Subset 30, Smooth 11,3, Thresh 0.5; Averaged over all images	
0.011	0.004	0.015	0.013	Subset 20, Smooth 11,3; Averaged over all images	
0.009	0.004	0.014	0.012	Subset 20+A9:I9, Smooth 11,3; Averaged over all images	
0.012	0.005	0.015	0.013	Subset 20, Smooth 11,3; Averaged over all images	
0.018	0.005	0.020	0.015	1 deg applied rotation	
0.034	0.010	0.037	0.028	2 deg applied rotation	Subset 20, Smooth 11,3; Averaged over center of image
0.050	0.016	0.057	0.045	3 deg applied rotation	
0.088	0.057	0.121	0.119	5 deg applied rotation	
0.017	0.005	0.019	0.014	1 deg applied rotation	
0.033	0.012	0.036	0.029	2 deg applied rotation	Subset 20, Smooth 11,3; Averaged over center of image
0.043	0.019	0.054	0.050	3 deg applied rotation	
0.073	0.052	0.096	0.110	5 deg applied rotation	
--	--	--	--	Analytic solution unknown.	
0.017	0.007	0.019	0.014	0.195 % applied strain	Subset 20, Smooth 11,3; Averaged over left and right portions of image, where strain is constant
0.014	0.007	0.039	0.026	0.391 % applied strain	
40.1*	2.1*	--	--	0.195 % applied strain	Subset 20, Smooth 11,3; *Width of the sharp strain discontinuity
54.4*	2.2*	--	--	0.391 % applied strain	
0.008	0.006	0.029	0.022	$1.8*10^{-3}$ pixels^{-1} average applied strain frequency	Subset 20, Smooth 11,3; Averaged over the right portion of the image, for X>1478
0.012	0.008	0.043	0.030	$5.3*10^{-3}$ pixels^{-1} average applied strain frequency	
0.023	0.013	0.130	0.075	$8.8*10^{-3}$ pixels^{-1} average applied strain frequency	
--	--	0.534	0.686	Ratio peak spacing to peak width = 0.24	Subset 20, Smooth 11,1; Averaged over the portion of the image where the applied strain is non-zero
--	--	0.315	0.562	Ratio peak spacing to peak width = 0.95	
--	--	0.202	0.378	Ratio peak spacing to peak width >1.19	

Sample 1 (TexGen Shift in X, Y with varying contrast)

Deformation: Rigid translation in both X and Y directions, with a step size of 0.05 pixels.

Images: 512 x 512 pixels. Varying contrast of images, but all images have a relatively good speckle pattern.

Results:
Using a threshold value of 0.5, all of the grid points correlated for all of the images (Fig. 2). The error in the displacements has a local minimum at 0.5 pixels of applied displacement (Fig. 3). The cause of this local minimum is unknown; it could be related to either the DIC code or to the image manipulation algorithm. The error in the raw correlated displacement values, averaged over the entire field of view for all images (except the self-correlation of the reference image), is approximately 0.05 +/- 0.04 pixels for a subset of 10 and 0.02 + 0.01 pixels for a subset of 20 (Fig. 5).

In theory, the raw displacements could be infinitely smoothed and a nearly-exact solution recovered since the deformation is rigid translation. However, in practice, if the data is smoothed too much, information on spatial variation will be lost. The smoothing parameters chosen in this section are similar to those chosen in the varying strain samples described in Samples 11, 14, and 15, and so are considered to be reasonable. Using a kernel size of 11 and smoothing 3 times provides the most reduction in error. A kernel size of 7 with 3 smoothing passes and a kernel size of 11 with 1 smoothing pass provide nearly identical reductions in error.

The average error in the strain values computed from the raw displacements is 1.5-2 % strain for a subset of 20 and 0.5-0.6 % strain for a subset of 10. These results emphasize the need for some smoothing of the raw displacements before computation of strains. The reduction of error in the calculated strains follows the same trend as the error in displacements with regard to the different smoothing parameters.
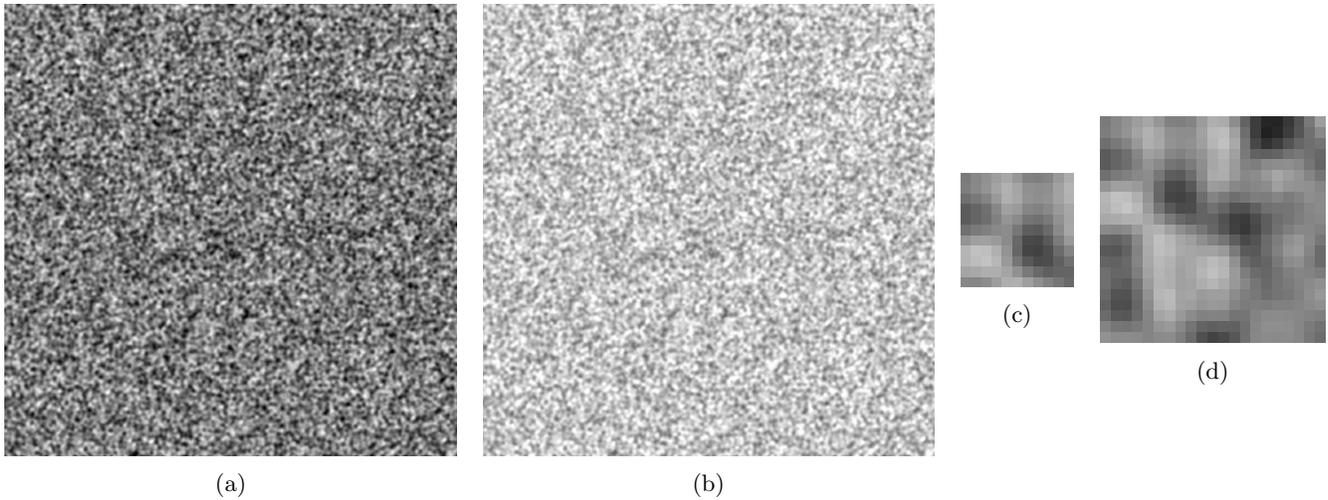
Figure 1: (a) Reference image and (b) final image. The contrast of the images decreases moving from the reference to the final image. (c-d) Representative subsets for subset size 10 and 20 respectively.
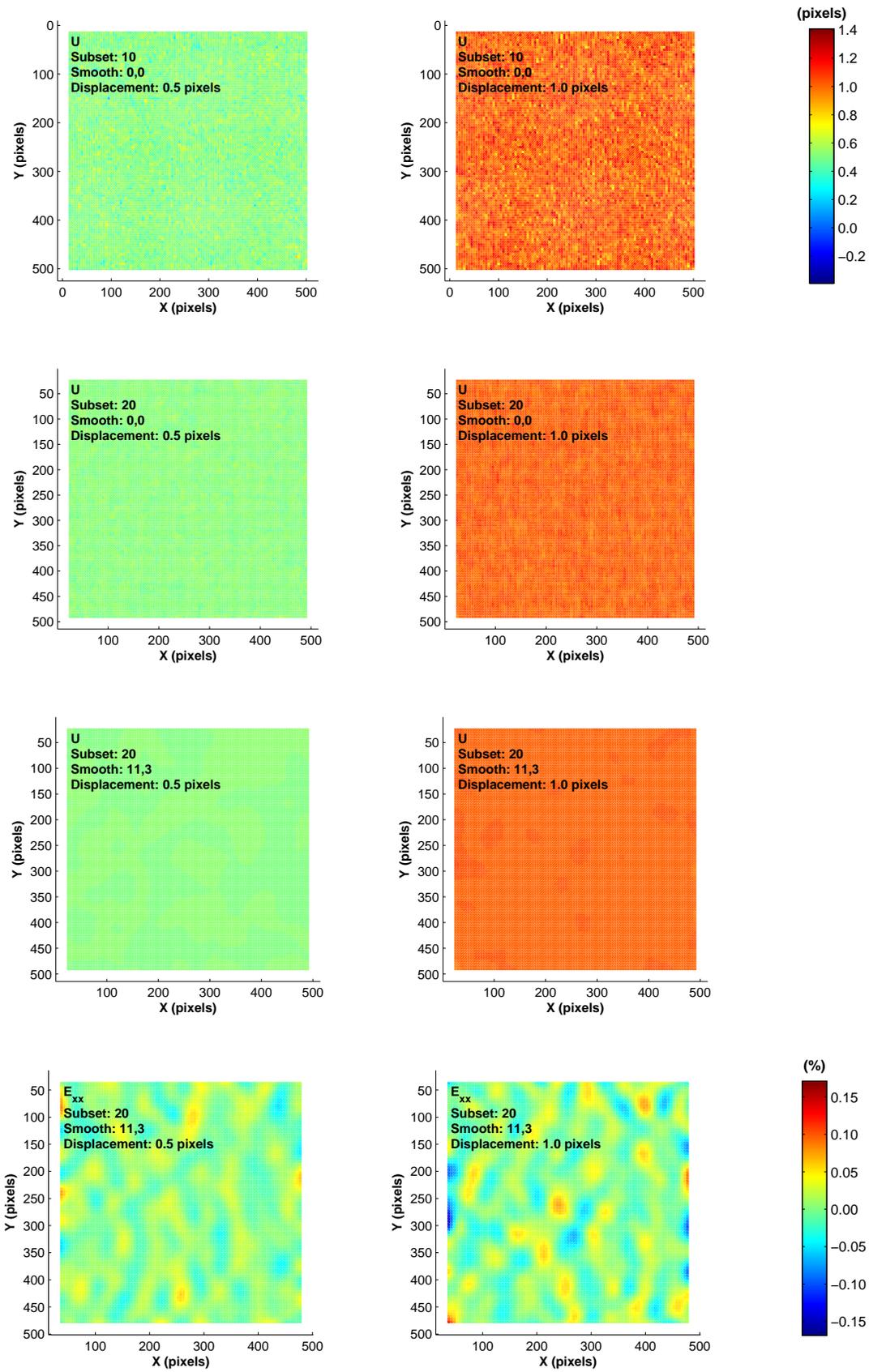
Figure 2: Select contour plots of the horizontal displacement, U, and the horizontal normal strain, E_{xx}.
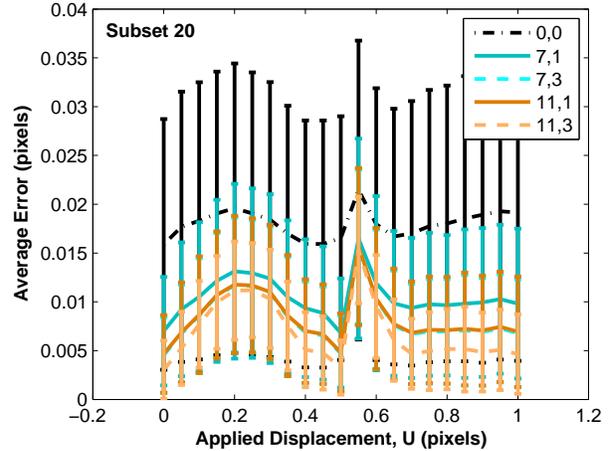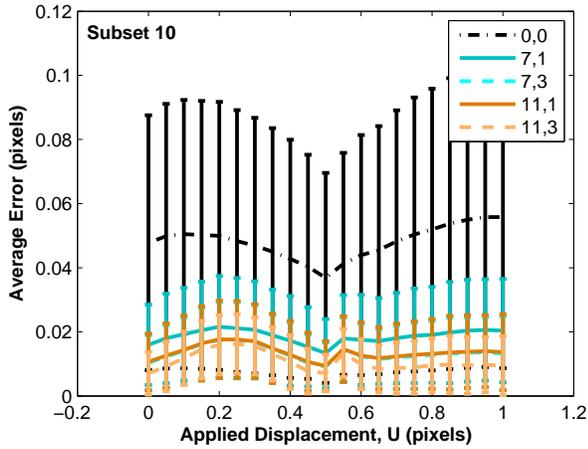
Figure 3: Error, averaged over the entire image, of the horizontal displacement, U, as a function of the applied horizontal displacement. The legend indicates different smoothing parameters as [smooth kernel size, number of smoothing passes]. The error bars represent one standard deviation.
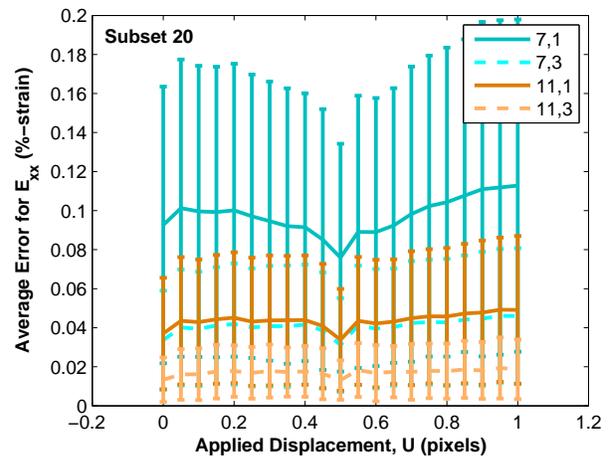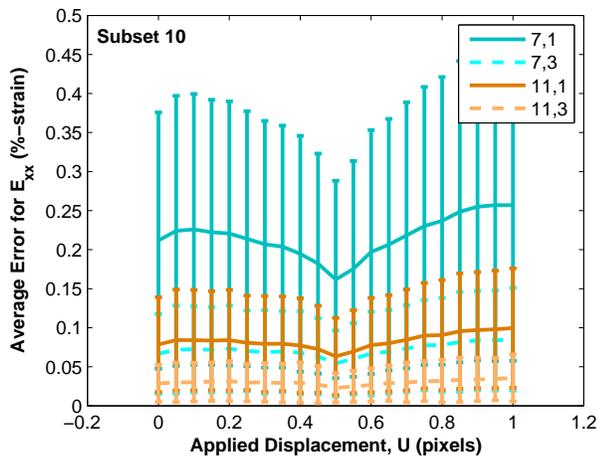

Figure 4: Error, averaged over the entire image, of the horizontal normal strain, E_{xx}, as a function of the applied horizontal displacement. The legend indicates different smoothing parameters as [smooth kernel size, number of smoothing passes]. The error bars represent one standard deviation.
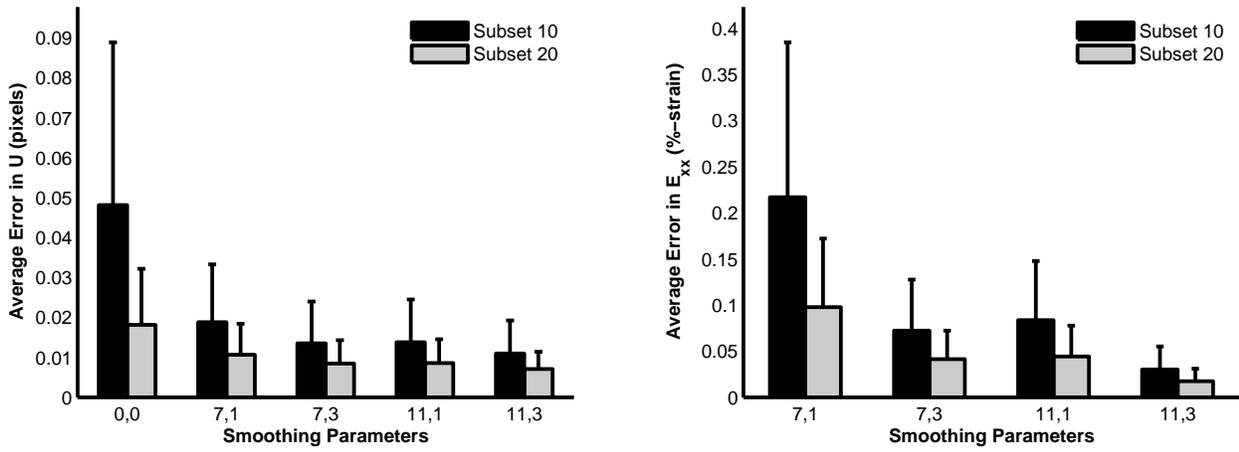
Figure 5: Error, averaged over all the images except for the self-correlation of the reference image, of the horizontal displacement, U, and the horizontal normal strain, E_{xx}, as a function of subset size and smoothing parameters. The smoothing parameters labeled on the x-axis are [smooth kernel size, number of smoothing passes]. The error bars represent one standard deviation.

Sample 2 (TexGen Shift in X, Y with low contrast)

Deformation: Rigid translation in both X and Y directions, with a step size of 0.05 pixels.

Images: 512 x 512 pixels. Poor quality speckle pattern; low contrast.

Results:

Compared to Sample 1, the speckle pattern in Sample 2 has low contrast and more blank space between identifiable features. Therefore, larger subset sizes (20 and 30) are evaluated in this section compared to the previous section.

Using a threshold of 0.50, on average 8 % of grid points did not correlate for a subset of 20, and an average of 2 % of grid points did not correlate for a subset of 30. For a subset of 30, less than 4 grid points (0.05 % of grid points) did not correlate when the threshold was reduced to 0.35, and all points correlated when the threshold was further reduced to 0.25 (Fig. 7). The errors in the raw displacements, smoothed displacements and strains are equivalent for all thresholds, given a subset of 30 (Fig 10). No improvement is observed by reducing the threshold to have more correlated points.

As a result of the poorer speckle pattern, the errors in the displacements are larger for Sample 2 compared to Sample 1. The same trends with regards to smoothing are observed in Sample 2 as in Sample 1. Given this speckle pattern, the parameters with the least error in the strain (subset 30, smooth 11,3, any threshold) still resulted in fairly large strain errors of approximately 0.2 %. Therefore, caution must be used when using this DIC code to correlate images with a poor speckle pattern.
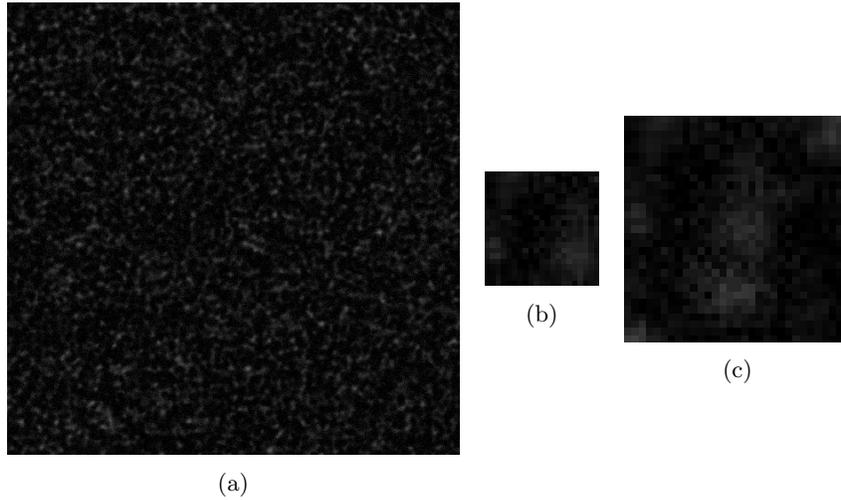
Figure 6: (a) Reference image. (b-c) Representative subsets for subset size 20 and 30 respectively.
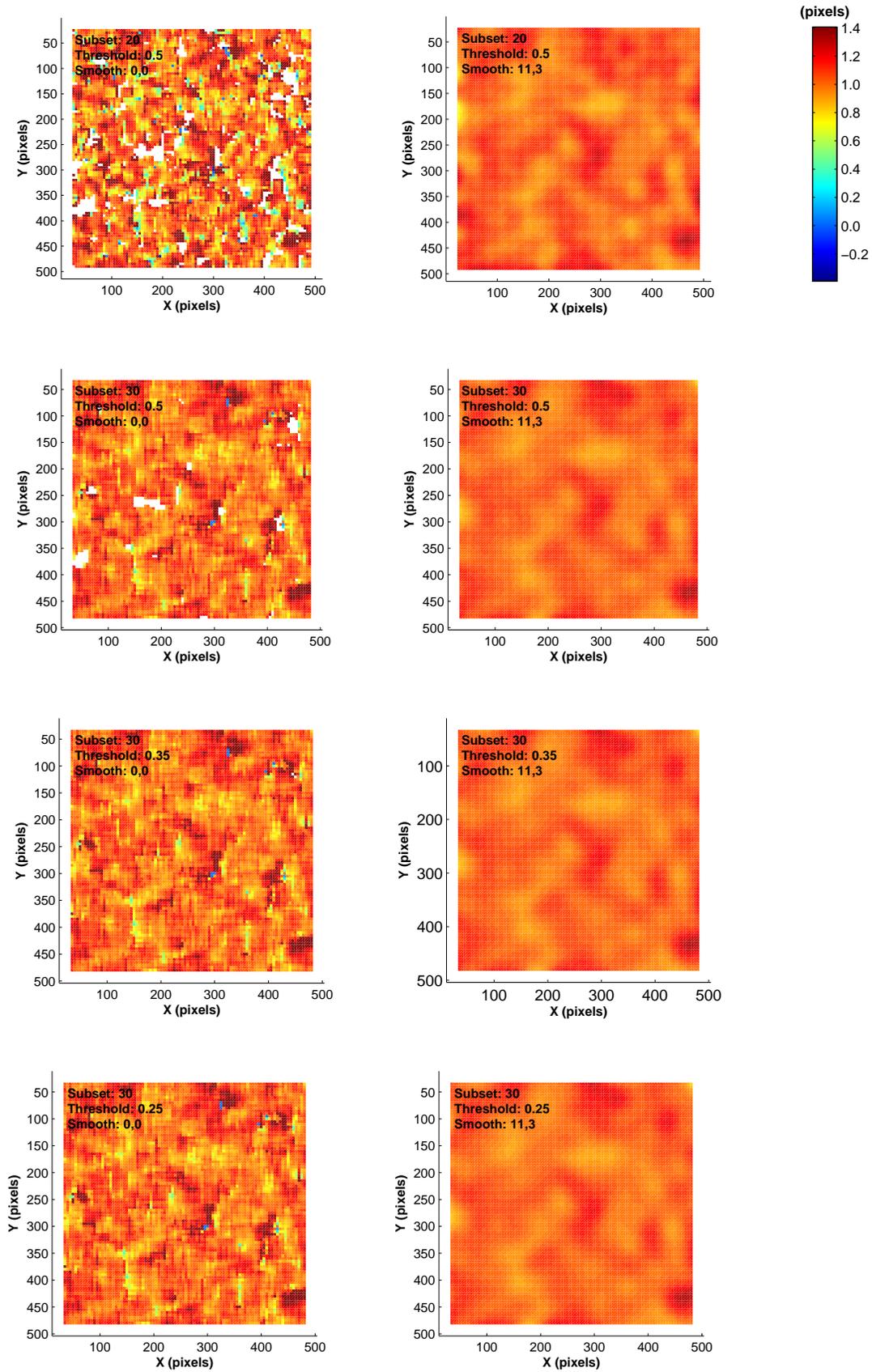
Figure 7: Select contour plots of the horizontal displacement, U, at the applied displacement of 1.00 pixel. Grid points that did not correlate are represented as white boxes in the contours of the unsmoothed displacements. The smoothing process extrapolates data from surrounding points in order to have displacement values at every grid point.

11
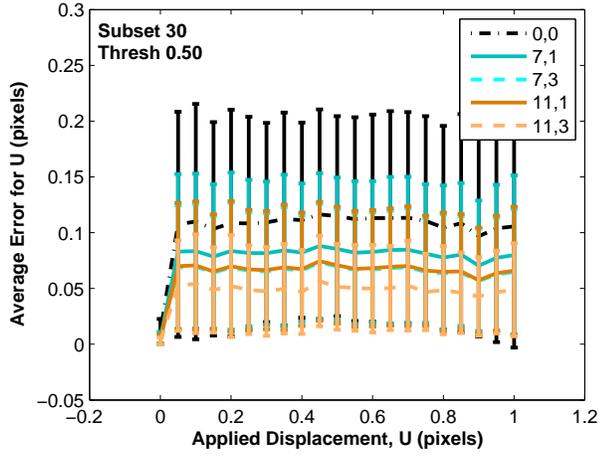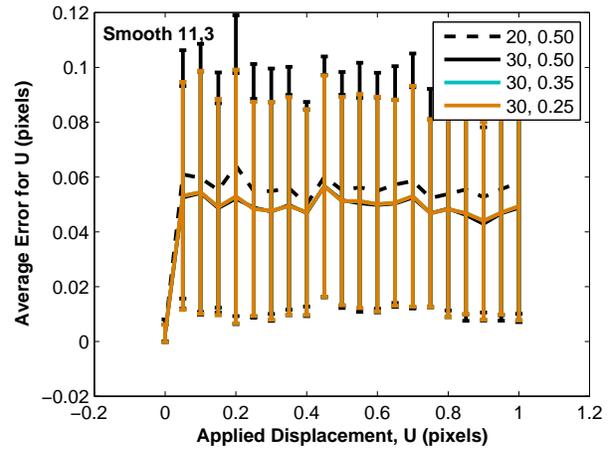
(a)   (b)

Figure 8: Error, averaged over the entire image, of the horizontal displacement, U, as a function of the applied horizontal displacement. The legend in (a) indicates different smoothing parameters as [smooth kernel size, number of smoothing passes]. The legend in (b) indicates [subset size, threshold value]. The error bars represent one standard deviation.
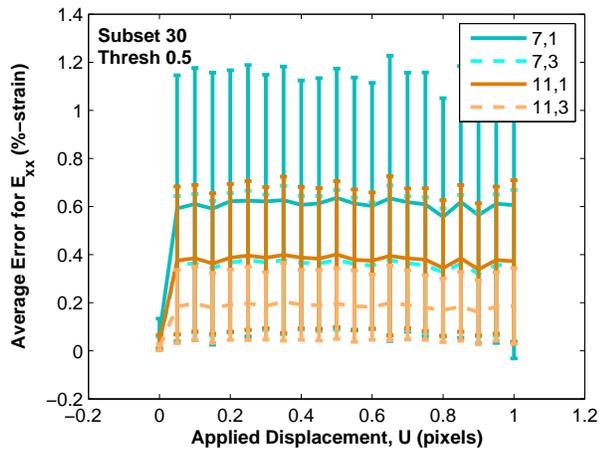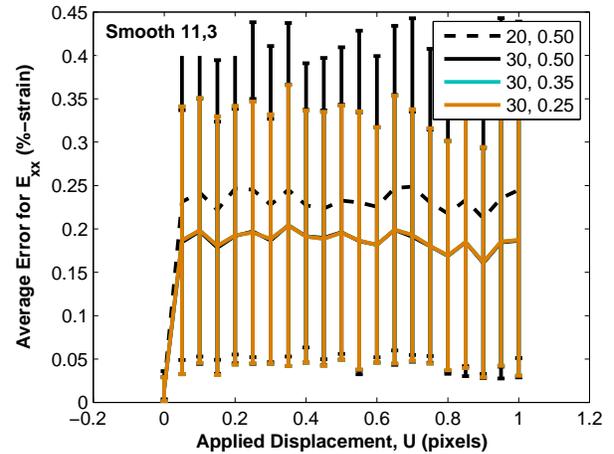
(a)   (b)

Figure 9: Error, averaged over the entire image, of the horizontal normal strain, E_{xx}, as a function of the applied horizontal displacement. The legend in (a) indicates different smoothing parameters as [smooth kernel size, number of smoothing passes]. The legend in (b) indicates [subset size, threshold value]. The error bars represent one standard deviation.
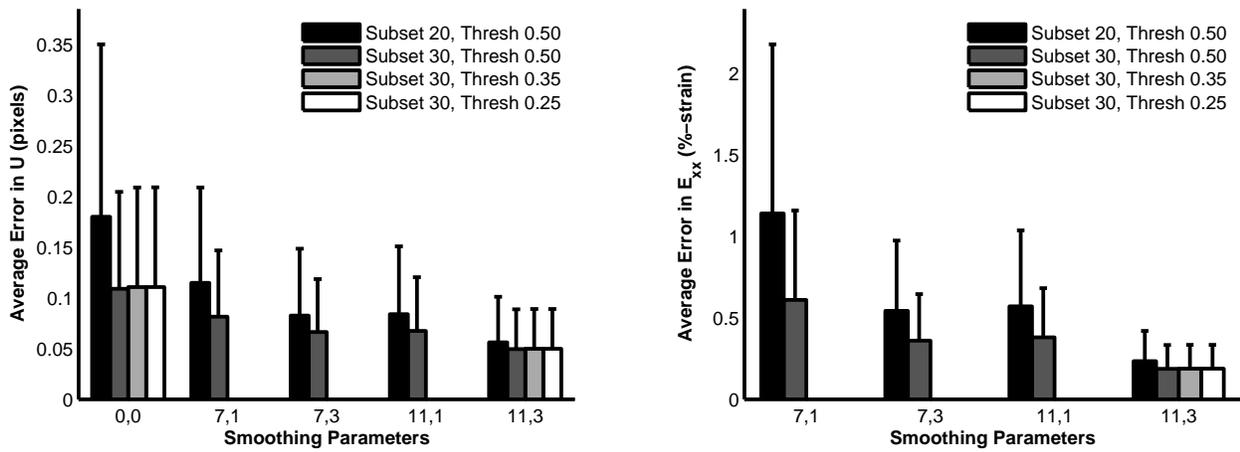
Figure 10: Error, averaged over all the images except for the self-correlation of the reference image, of the horizontal displacement, U, and the horizontal normal strain, E_{xx}, as a function of subset size, threshold value, and smoothing parameters. The smoothing parameters labeled on the x-axis are [smooth kernel size, number of smoothing passes]. The error bars represent one standard deviation.

Sample 3 (FFT Shift in X, Y)

Deformation: Rigid translation in both X and Y directions, with a step size of 0.10 pixels.

Images: 512 x 512 pixels. Constant and relatively good speckle pattern for all images.

Results:
The results of Sample 3 are similar to those of Sample 1.

(a)

(b)

(c)
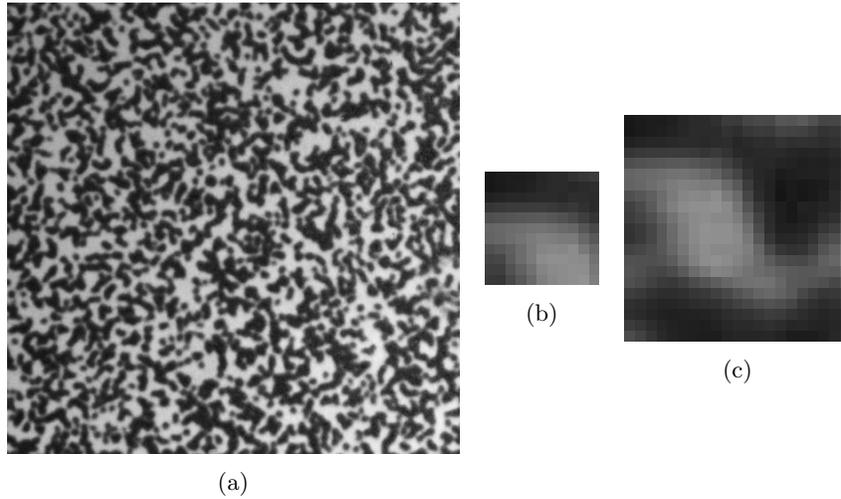
Figure 11: (a) Reference image. (b-c) Representative subsets for subset size 10 and 20 respectively.
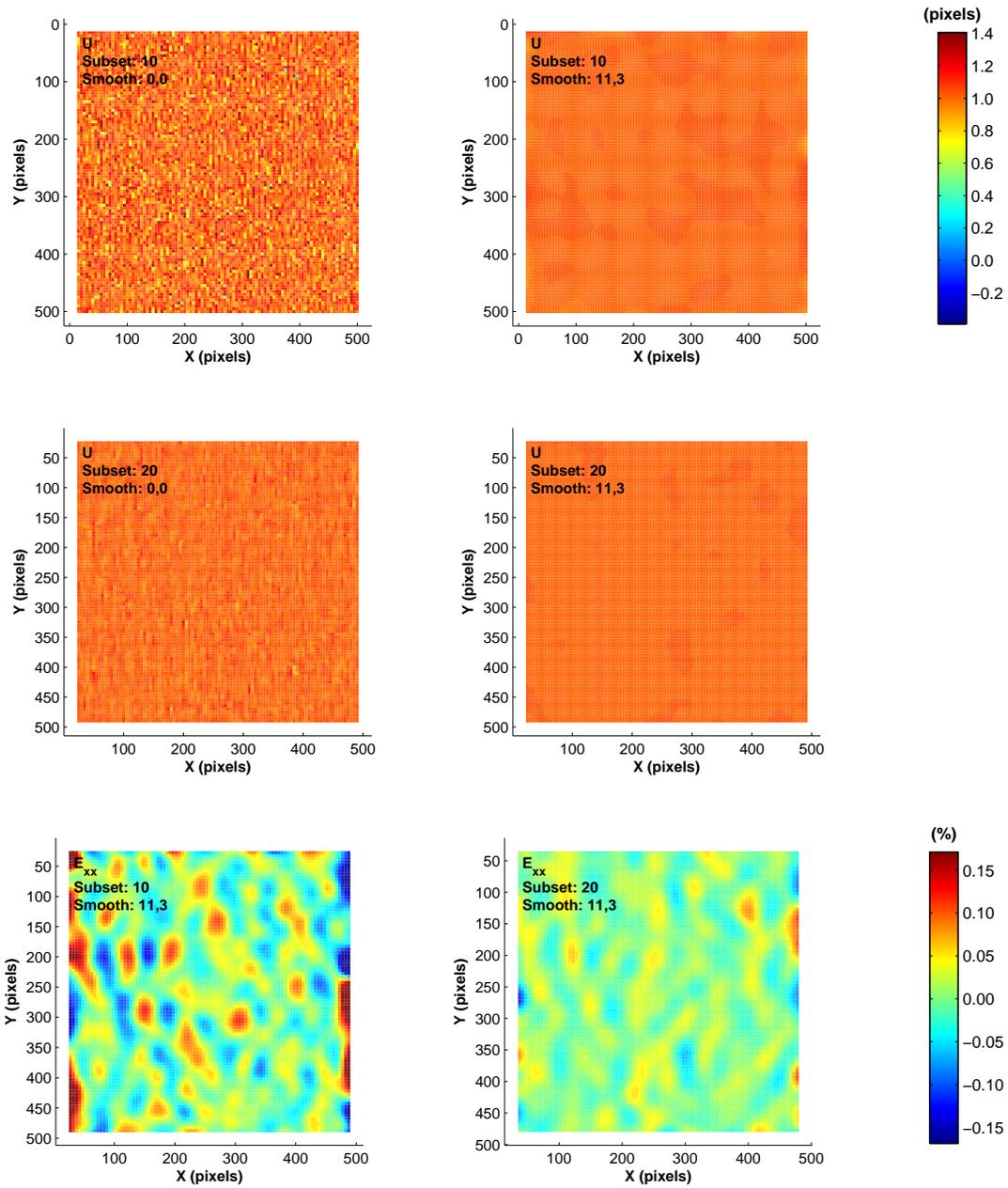
Figure 12: Select contour plots of the horizontal displacement, U, and horizontal normal strain, E_{xx}, at the applied horizontal displacement of 1.00 pixel.
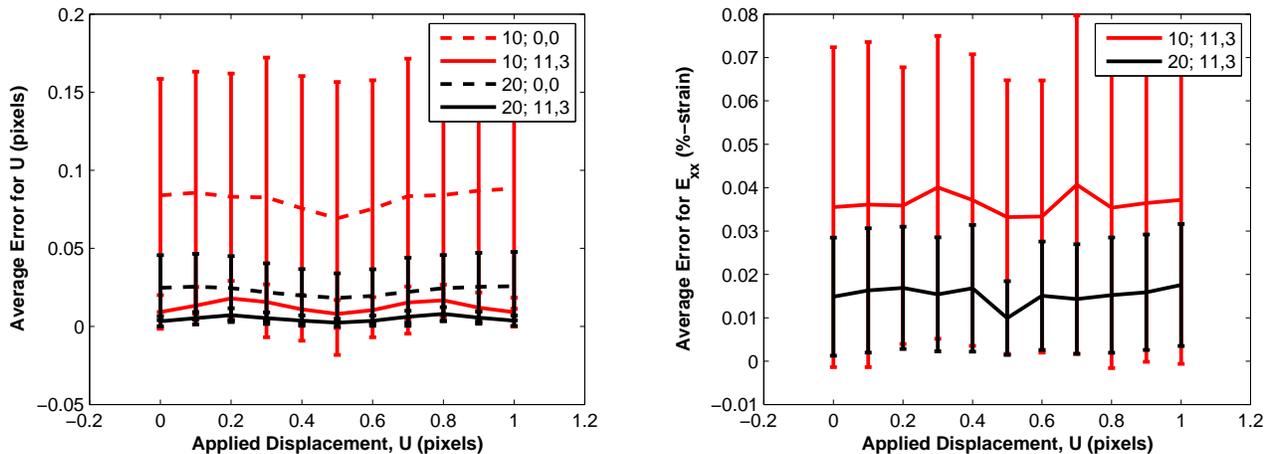
Figure 13: Error, averaged over the entire image, of the horizontal displacement, U, and the horizontal normal strain, E_{xx}, as a function of the applied horizontal displacement. The legend indicates correlation and smoothing parameters as [subset size; smooth kernel size, number of smoothing passes]. The error bars represent one standard deviation.
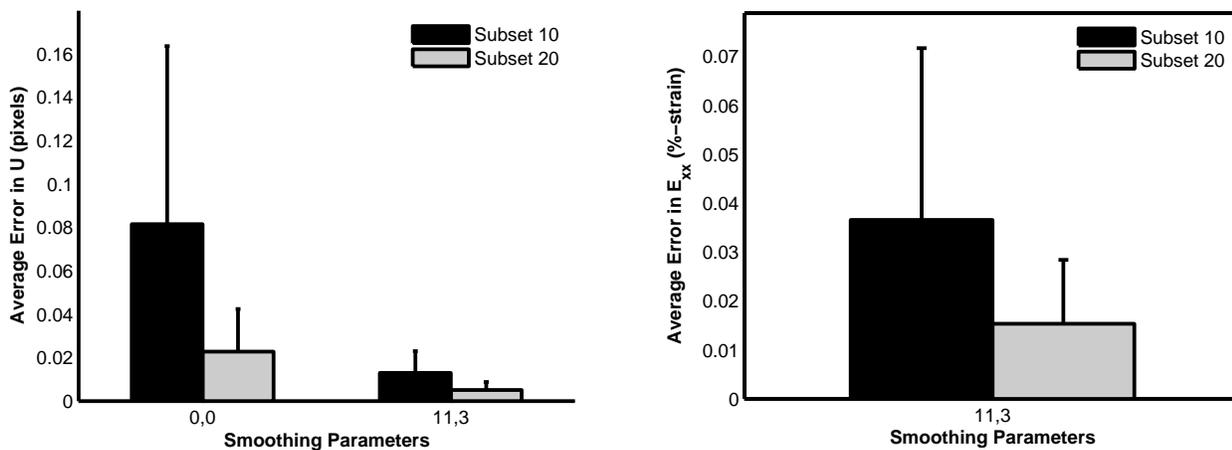
Figure 14: Error, averaged over all the images except for the self-correlation of the reference image, of the horizontal displacement, U, and the horizontal normal strain, E_{xx}, as a function of subset size and smoothing parameters. The smoothing parameters labeled on the x-axis are [smooth kernel size, number of smoothing passes]. The error bars represent one standard deviation.

Sample 4 (FFT Shift in X, Y with low contrast)

Deformation: Rigid translation in both X and Y directions, with a step size of 0.10 pixels.

Images: 512 x 512 pixels. Poor speckle pattern; low contrast.

Results:
The results of Sample 4 are similar to those of Sample 2, which also had a poor quality speckle pattern.
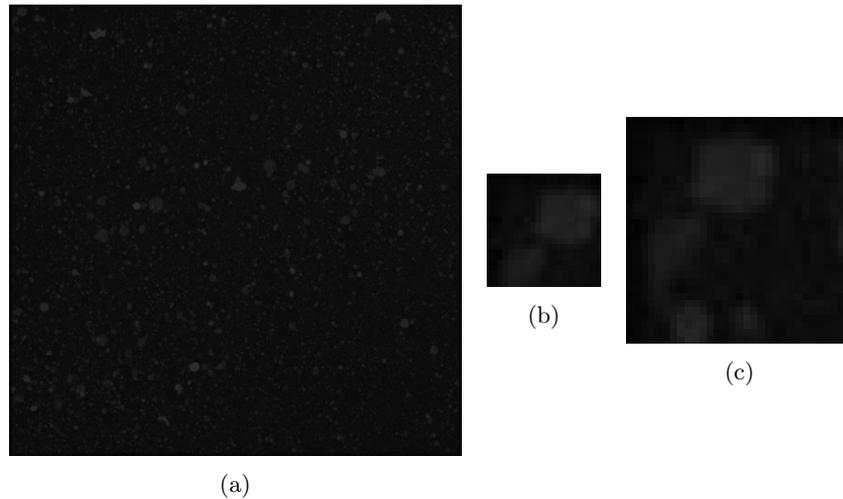

Figure 15: (a) Reference image. Representative subsets for (b) subset size 20 (b) and (c) subset size 30.
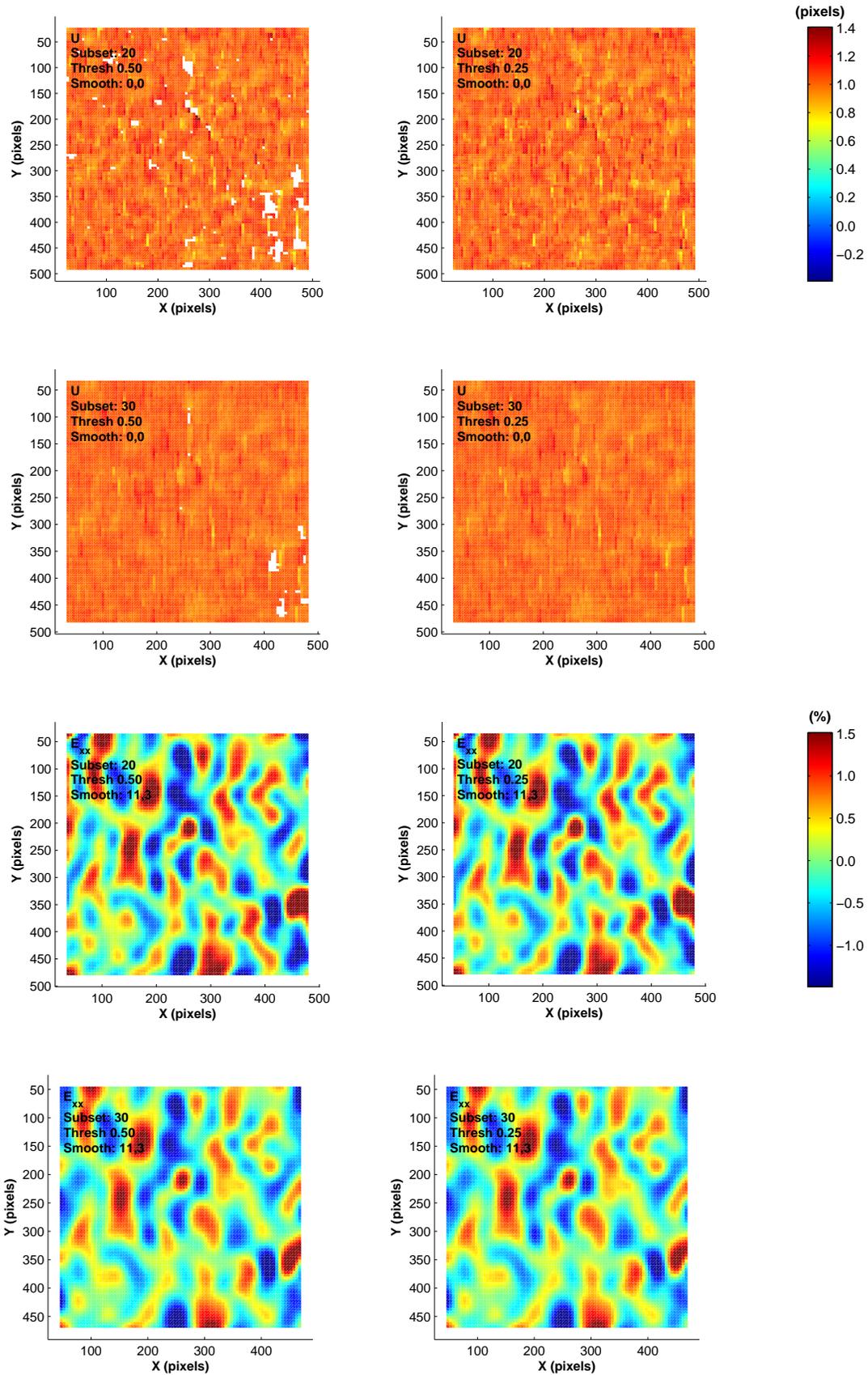
Figure 16: Select contour plots of the horizontal displacement, U, and the horizontal normal strain, E_{xx}, at the applied displacement of 1.00 pixel. Grid points that did not correlate are represented as white boxes in the contours of the unsmoothed displacements. The smoothing process extrapolates data from surrounding points in order to have displacement values at every grid point.

18
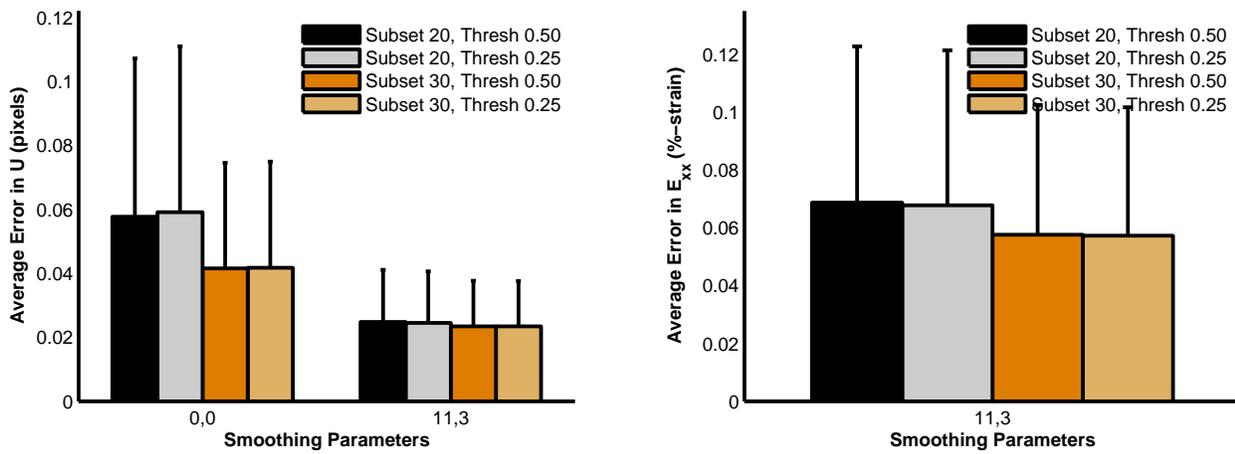
Figure 17: Error, averaged over all the images except for the self-correlation of the reference image, of the horizontal displacement, U, and the horizontal normal strain, E_{xx}, as a function of subset size, threshold value, and smoothing parameters. The smoothing parameters labeled on the x-axis are [smooth kernel size, number of smoothing passes]. The error bars represent one standard deviation.

Sample 5 (FFT Shift in X, Y with varying contrast)

Deformation: Rigid translation in both X and Y directions, with a step size of 0.1 pixels.

Images: 512 x 512 pixels. Varying contrast of images, but all images have a relatively good speckle pattern.

Results:
    The results of Sample 5 are similar to those of Samples 1 and 3.
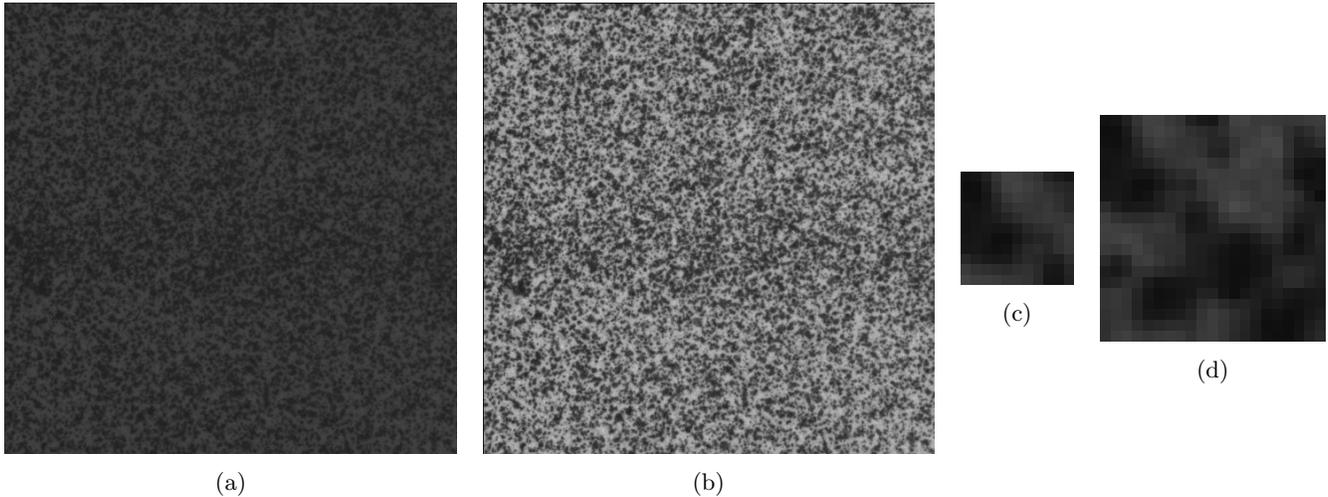
Figure 18: (a) Image with the poorest contrast (image 8), (b) image with the best contrast (image 11), (c-d) reference image (image 1) with subset size of 10 and 20 respectively.
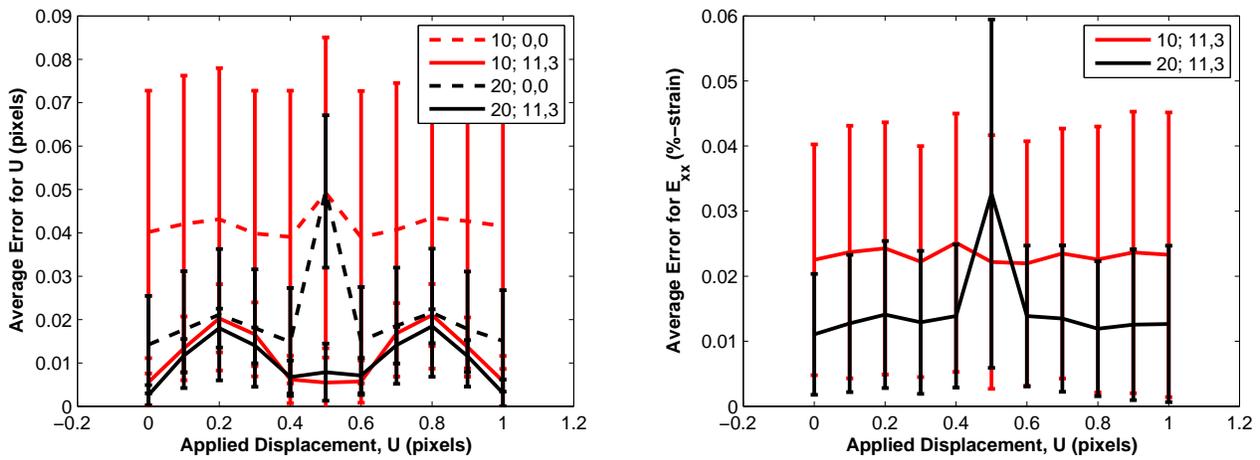
Figure 19: Error, averaged over the entire image, of the horizontal displacement, U, and the horizontal normal strain, E_{xx}, as a function of the applied horizontal displacement. The legend indicates correlation and smoothing parameters as [subset size; smooth kernel size, number of smoothing passes]. The error bars represent one standard deviation.
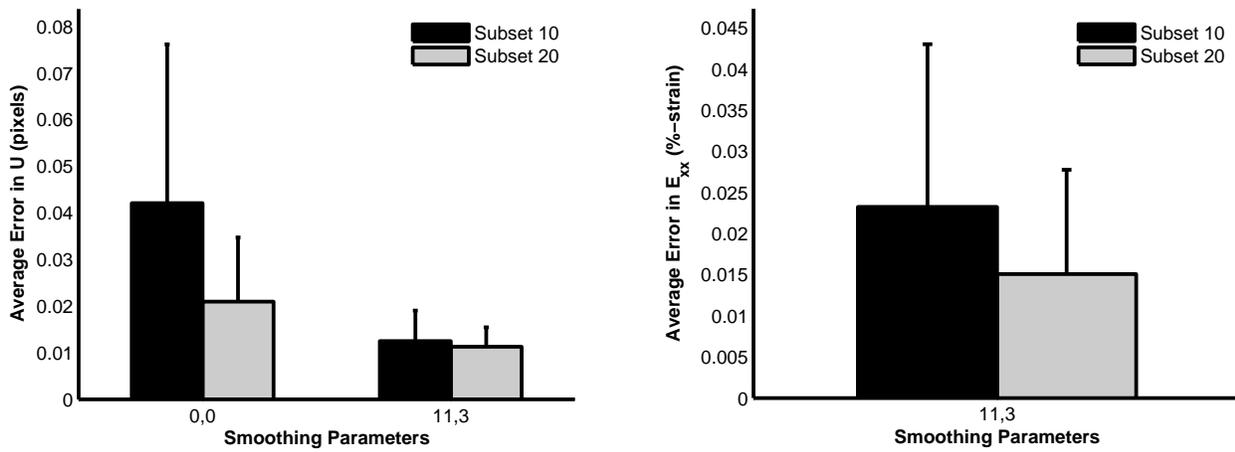
Figure 20: Error, averaged over all the images except for the self-correlation of the reference image, of the horizontal displacement, U, and the horizontal normal strain, E_{xx}, as a function of subset size and smoothing parameters. The smoothing parameters labeled on the x-axis are [smooth kernel size, number of smoothing passes]. The error bars represent one standard deviation.

Sample 6 (Prosilica Bin Shift in X, Y)

Deformation: Rigid translation in both X and Y directions, with a step size of 0.1 pixels.

Images: 487 x 325 pixels. Isolated dot speckle pattern.

Results:

The results of Sample 6 are similar to those of Samples 1, 3, and 5.


(a)

(b)
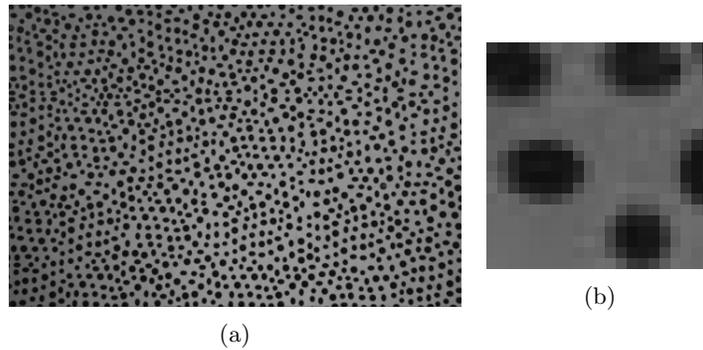
Figure 21: (a) Reference image. (b) Representative subset for subset size 20.
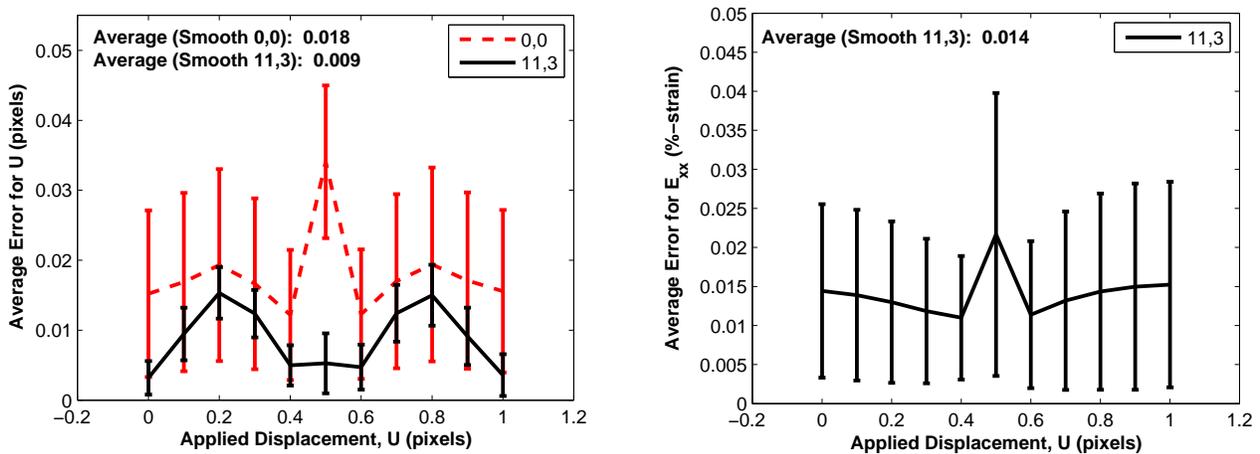
Figure 22: Error, averaged over the entire image, of the horizontal displacement, U, and the horizontal normal strain, E_{xx}, as a function of the applied horizontal displacement. A subset size of 20 was used for these correlations. The legend indicates smoothing parameters as [subset size; smooth kernel size, number of smoothing passes]. The note in the top-left corner gives the error averaged over all images except for the self-correlation of the reference image. The error bars represent one standard deviation.

Sample 7 (Prosilica Bin Shift in X, Y)

Deformation: Rigid translation in both X and Y directions, with a step size of 0.1 pixels.

Images: 487 x 325 pixels. Good speckle pattern.

Results:

The results of Sample 7 are similar to those of Samples 1, 3, 5, and 6.
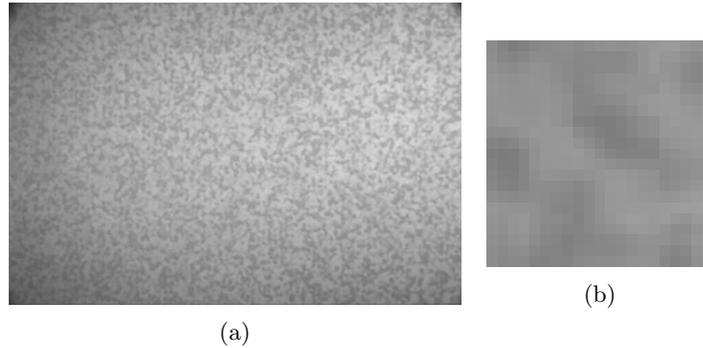
Figure 23: (a) Reference image. (b) Representative subset for subset size 20.
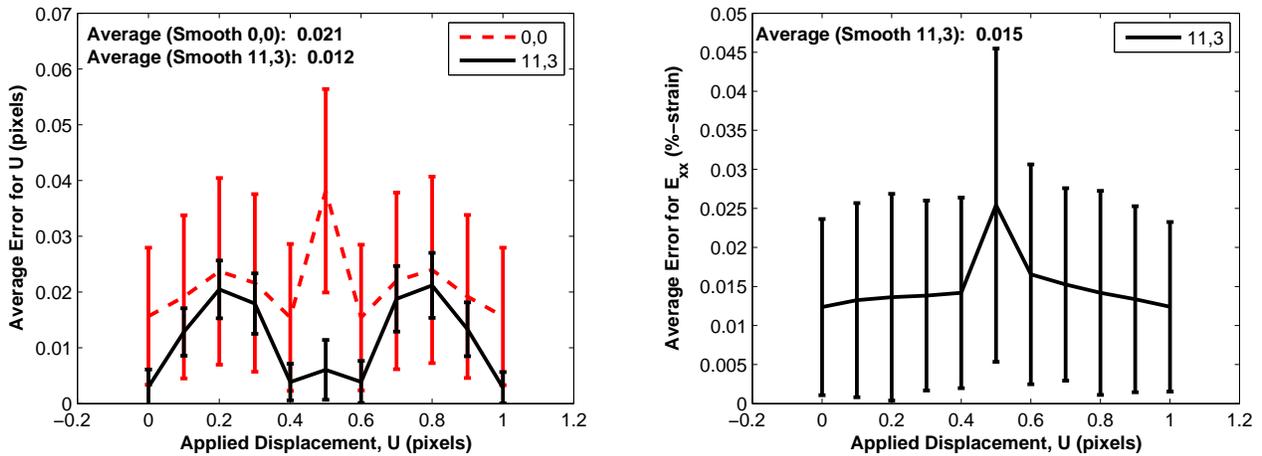

Figure 24: Error, averaged over the entire image, of the horizontal displacement, U, and the horizontal normal strain, E_{xx}, as a function of the applied horizontal displacement. A subset size of 20 was used for these correlations. The legend indicates smoothing parameters as [subset size; smooth kernel size, number of smoothing passes]. The note in the top-left corner gives the error averaged over all images except for the self-correlation of the reference image. The error bars represent one standard deviation.

Sample 8 (TexGen Rotation)

Deformation: Rigid body rotation about the center of the image in 1 deg increments from 0 deg to 9 deg.

Images: 512 x 512 pixels. Constant speckle pattern.

Results:
Because the rotations induce large displacements (compared to the rigid body translations in image sets 1-4), the reduced images were correlated first to provide initial guesses for the full correlation. For all the analyses presented in this section, the same reduced correlation results were used, with the following parameters: reduction of 3, one reduced correlation, subset of 20 and threshold of 0.25. The effect of using initial guesses is seen most clearly in the contour plots of the difference between the analytic and raw correlated displacements for the largest rotation (Figs. 27 - 27); in these contour plots, the error follows a block pattern that relates to the location of the the grid points used for the reduced correlation.

For all applied rotations, the edges of the images rotate out of the field of view. For rotations smaller than approximately 6 deg, the border between the grid points closest to the image edge and the image edge itself is sufficient that all of the grid points are correlated. For larger rotations, however, grid points near the image edge leave the field of view and cannot be correlated (Figs. 27 - 27). The error of the smoothed correlated displacements are largest where the grid points did not correlate, because of the large area over which displacements were extrapolated (Figs. 27 - 27).

For a more accurate picture of the error associate purely with the rotations (ignoring error associated with grid points leaving the field of view and not correlating), the error is averaged over the center of the field of view, where $100 < X < 412$ and $100 < Y < 412$ (i.e. discounting any grid points that are within 100 pixels from the image edges). The average error for both the displacements and the strains increases monotonically with applied rotation (Fig. 29). Therefore, caution must be exercised when using this DIC code in situations in which the test sample undergoes large rotations.


(a)

(b)

(c)
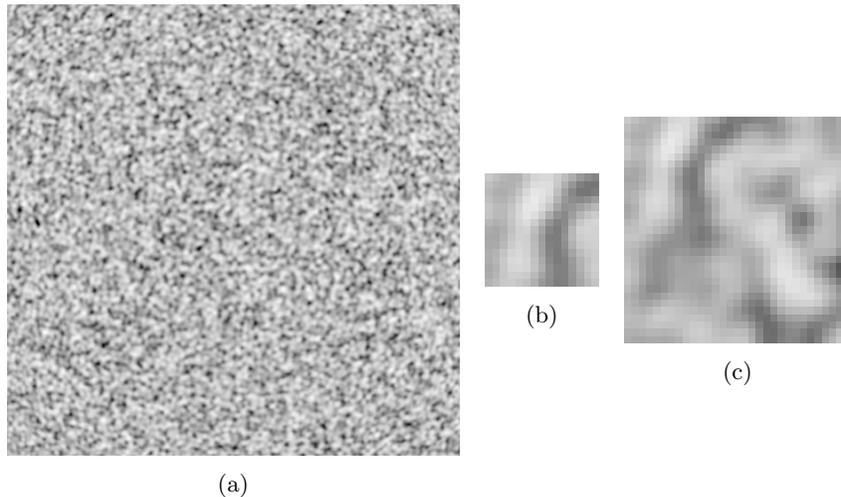
Figure 25: (a) Reference image. (b-c) Representative subsets for subset size 20 and subset size 30 respectively.
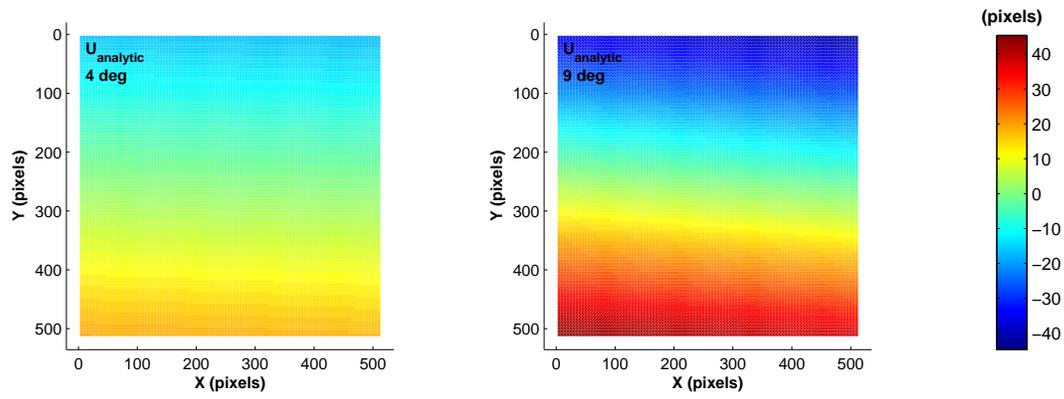
Figure 26: Contour plots of the analytical horizontal displacement, U, at 4 deg and 9 deg rotations.
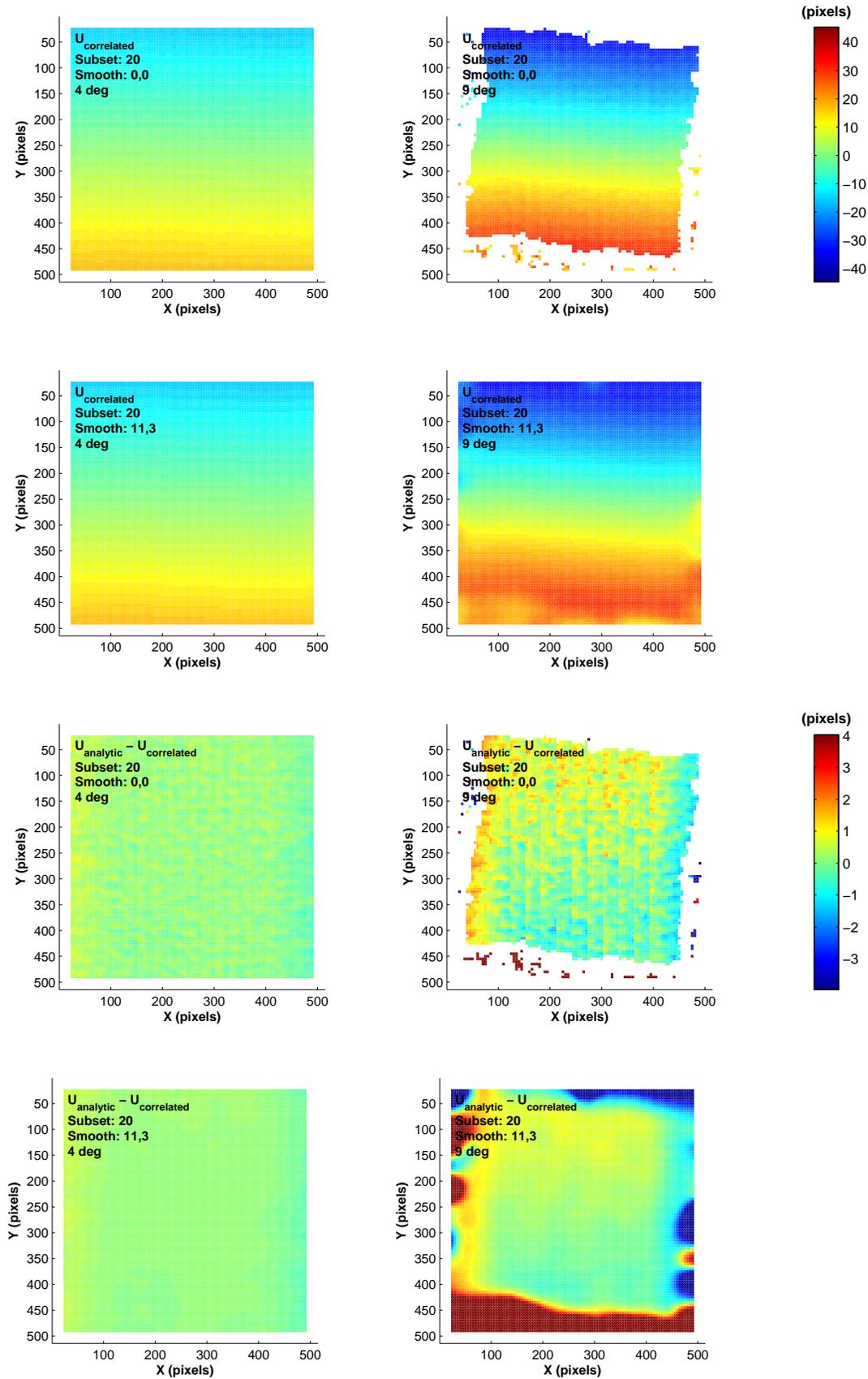
Figure 27: Select contour plots of the correlated horizontal displacement, $U_{correlated}$, (subset 20) and the difference between the correlated displacement and the analytic displacement, $U_{analytic}$ - $U_{correlated}$, at applied rotations of 4 deg and 5 deg. Grid points that did not correlate are represented as white boxes in the contours of the unsmoothed displacements. The smoothing process extrapolates data from surrounding points in order to have displacement values at every grid point.
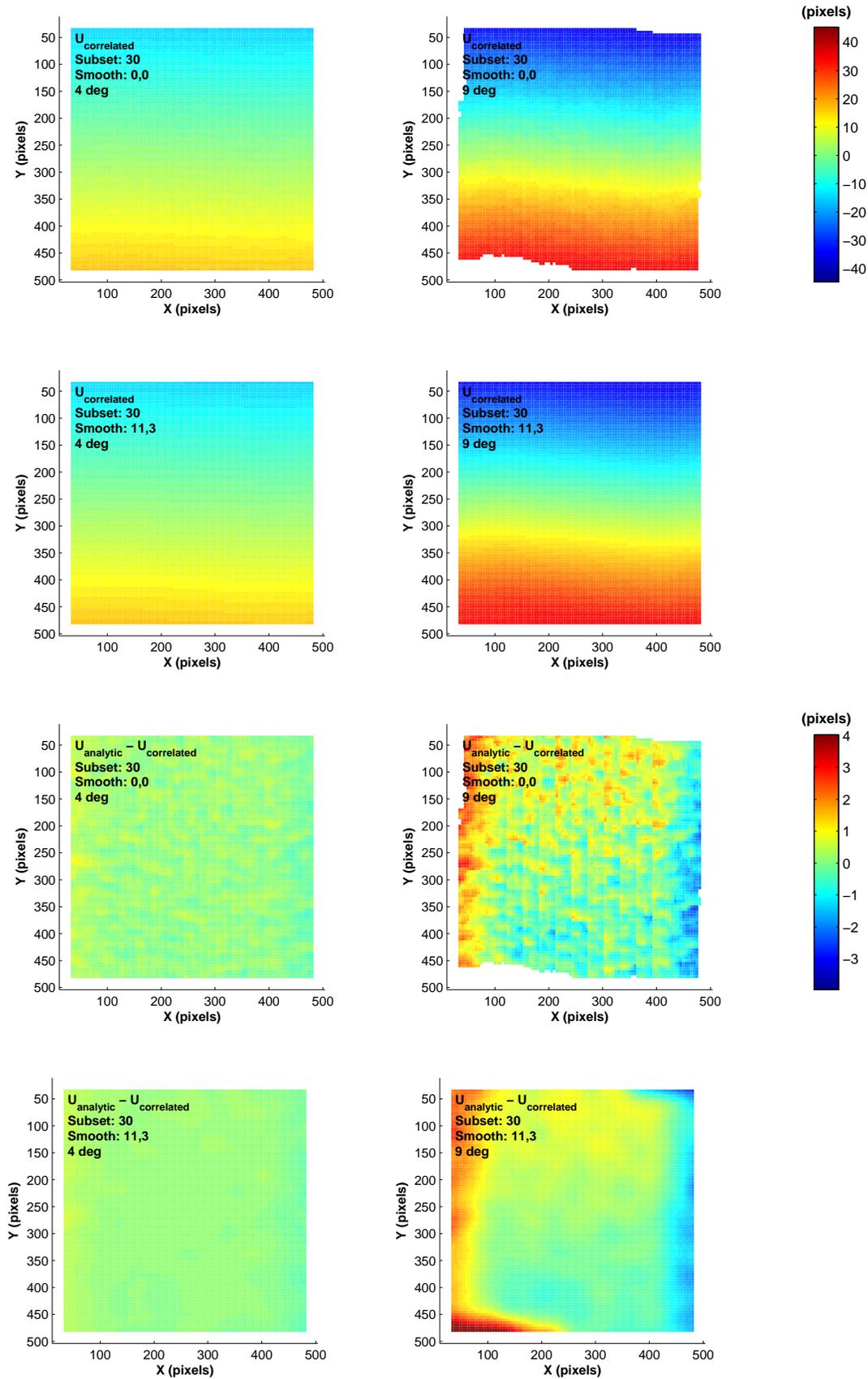
Figure 28: Select contour plots of the correlated horizontal displacement, U$_{correlated}$, (subset 30) and the difference between the correlated displacement and the analytic displacement, U$_{analytic}$ - U$_{correlated}$, at applied rotations of 4 deg and 5 deg. Grid points that did not correlate are represented as white boxes in the contours of the unsmoothed displacements. The smoothing process extrapolates data from surrounding points in order to have displacement values at every grid point.
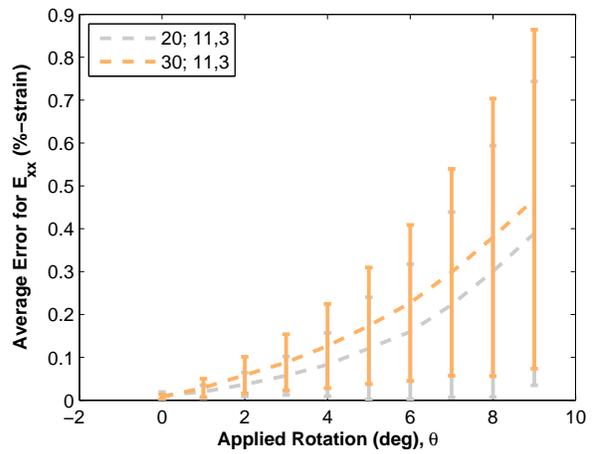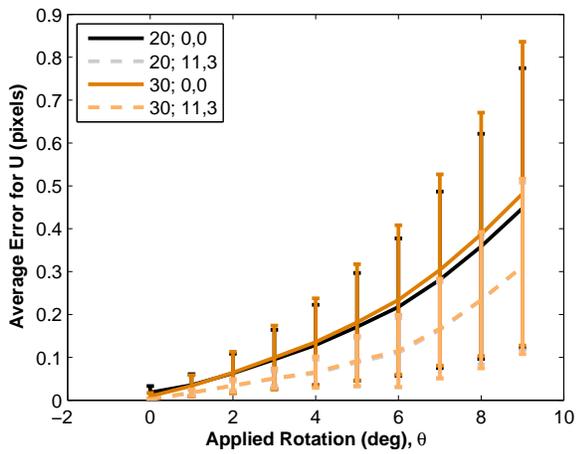
Figure 29: Error of horizontal displacement, U, and horizontal normal strain, E_{xx}, as a function of applied rotation. The error was averaged over the center of the field of view, where $100 < X < 412$ and $100 < Y < 412$, to avoid contribution to the error from grid points that rotated out of the field of view. The legend indicates the correlation and smoothing parameters as [subset size; smooth kernel size, number of smoothing passes]. The error bars represent one standard deviation.

Sample 9 (FFT Rotation)

Deformation: Rigid body rotation about the center of the image in 1 deg increments from 0 deg to 9 deg.

Images: 512 x 512 pixels. Constant speckle pattern.

Results:
The correlation results of Sample 9 are similar to those from Sample 8.
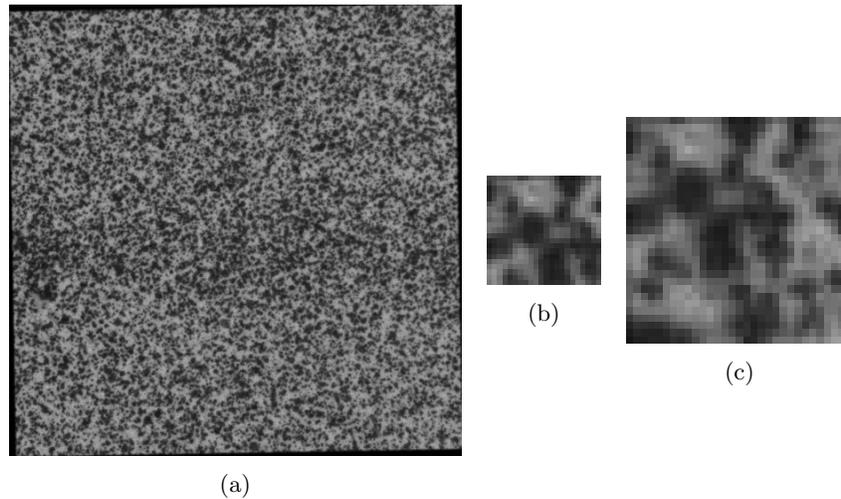
Figure 30: (a) Reference image. (b-c) Representative subsets for subset size 20 and 30 respectively.
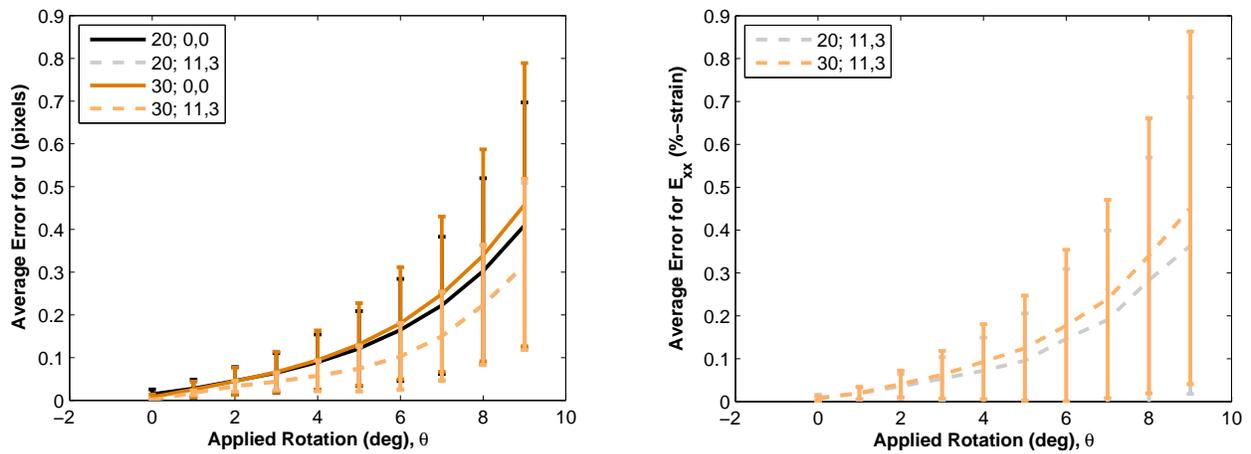

Figure 31: Error of horizontal displacement, U, and horizontal normal strain, E_{xx}, as a function of applied rotation. The error was averaged over the center of the field of view, where $100 < X < 412$ and $100 < Y < 412$, to avoid contribution to the error from grid points that rotated out of the field of view. The legend indicates the correlation and smoothing parameters as [subset size; smooth kernel size, number of smoothing passes]. The error bars represent one standard deviation.

Sample 10 (Large Strain)

Deformation: Large displacements and strains in the vertical direction. Exact analytic solution is unknown.

Images: 512 x 512 pixels. Good speckle pattern initially but large strain stretches speckle pattern significantly in the vertical direction.

Results:

This image set has two challenges: large displacements and a stretched speckle pattern. The first challenge of large displacements is addressed by correlating the reduced images to provide initial guesses for the correlation of the full images. The second challenge of a stretched speckle pattern is addressed by performing incremental correlations in which the preceding image, instead of the first image, is used as the reference image; changing the reference image for each image minimizes the distortion of the speckle pattern between the reference image and the image being correlated. Typically, using initial guesses and using the preceding image as a reference image would provide satisfactory correlation results. For this particular image set, however, there are still many points that are not correlated for the last image. Reducing the threshold value has no effect, as the points that did not correlate have a correlation coefficient of either 0 (because the control points moved out of the image) or -1 (because the correlated displacement is greater than the maximum allowed by the code). To address the latter set of control points, the search zone was increased from 2 to 4. Increasing the search zone allowed more control points in the center of the image to be successfully correlated, but at the expense of requiring a larger border between the edge control points and the edge of the image. The contour plots in Figs. 33 - 35 demonstrate the effect on the correlation results of changing the reference image, using (or not using) initial guesses, and changing the search zone.


(a) (b) (c) (d)
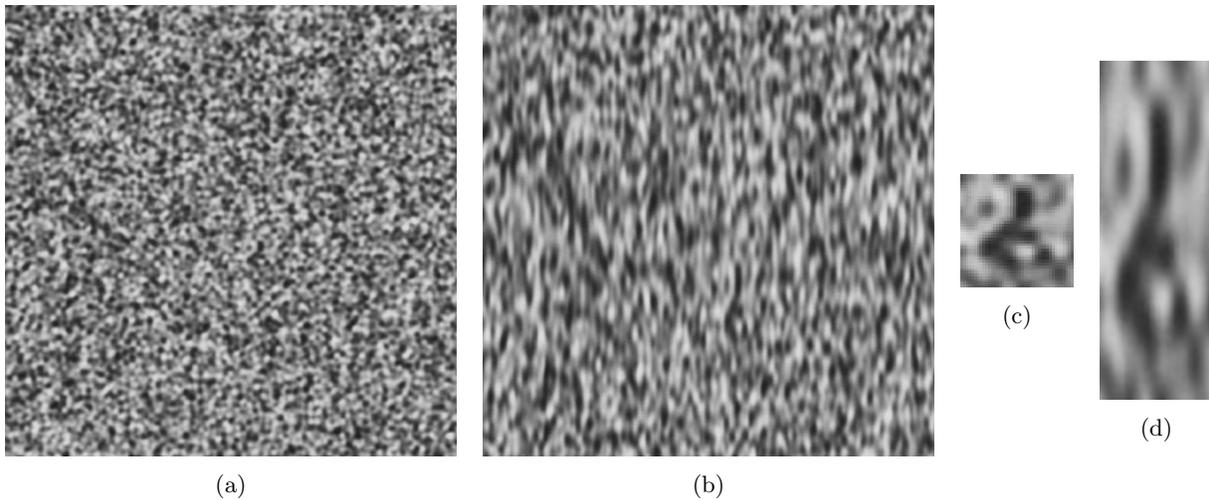
Figure 32: (a) Reference image and (b) final image. The speckle pattern is stretched significantly in the vertical direction moving from the reference to the final image. (c) Representative subset in the reference image for a subset size of 41 x 41 pixels. (d) Approximately the same subset in the final image; the height of the subset is 123 pixels instead of 41 pixels to emphasize the distortion in the speckle pattern.
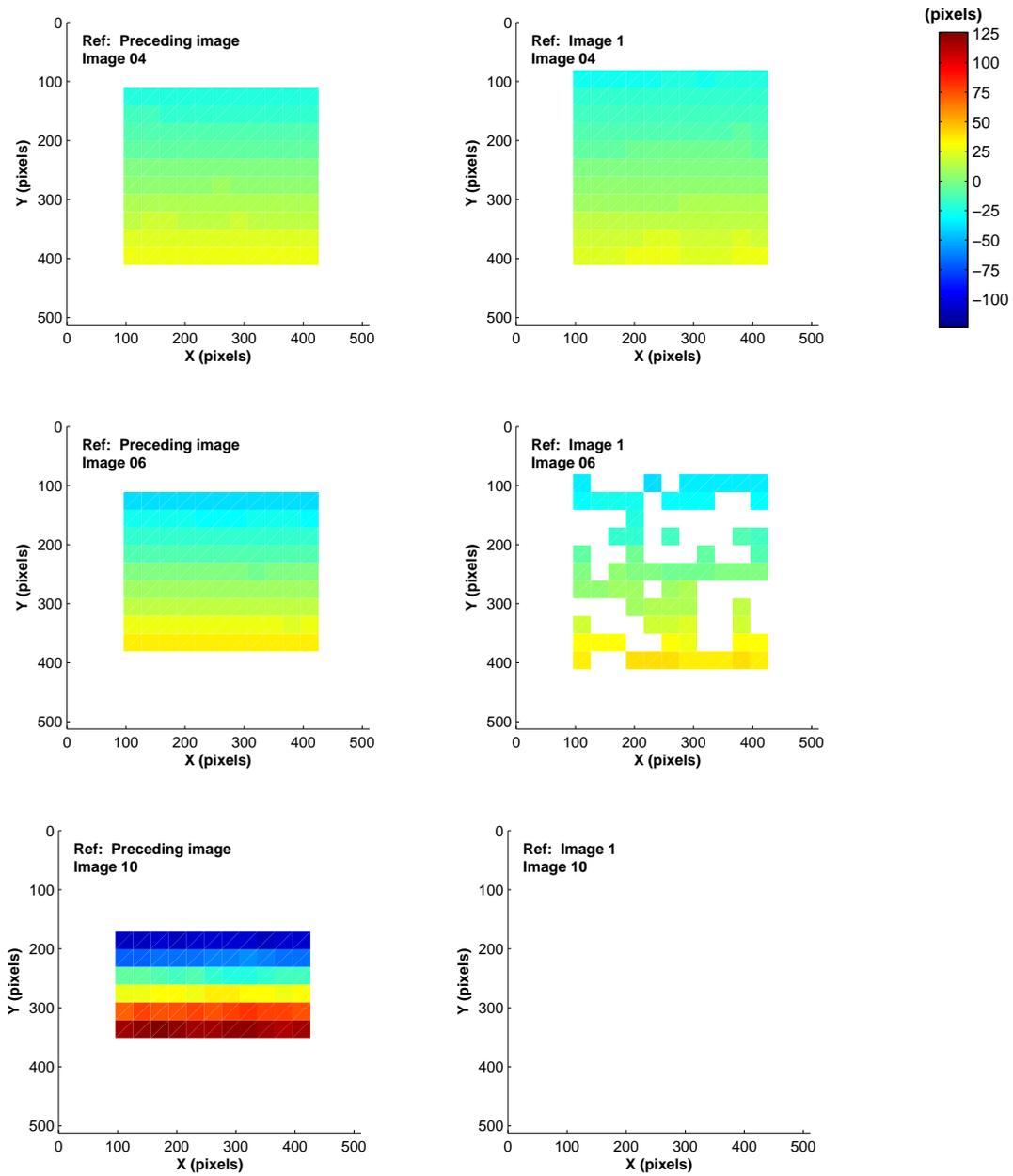
Figure 33: Select contour plots of the vertical displacement, V, from the correlation of the reduced images. The left column represents the correlation results when the preceding image was used as a reference image and the right column represents the correlation results when the first image was used as a reference image.
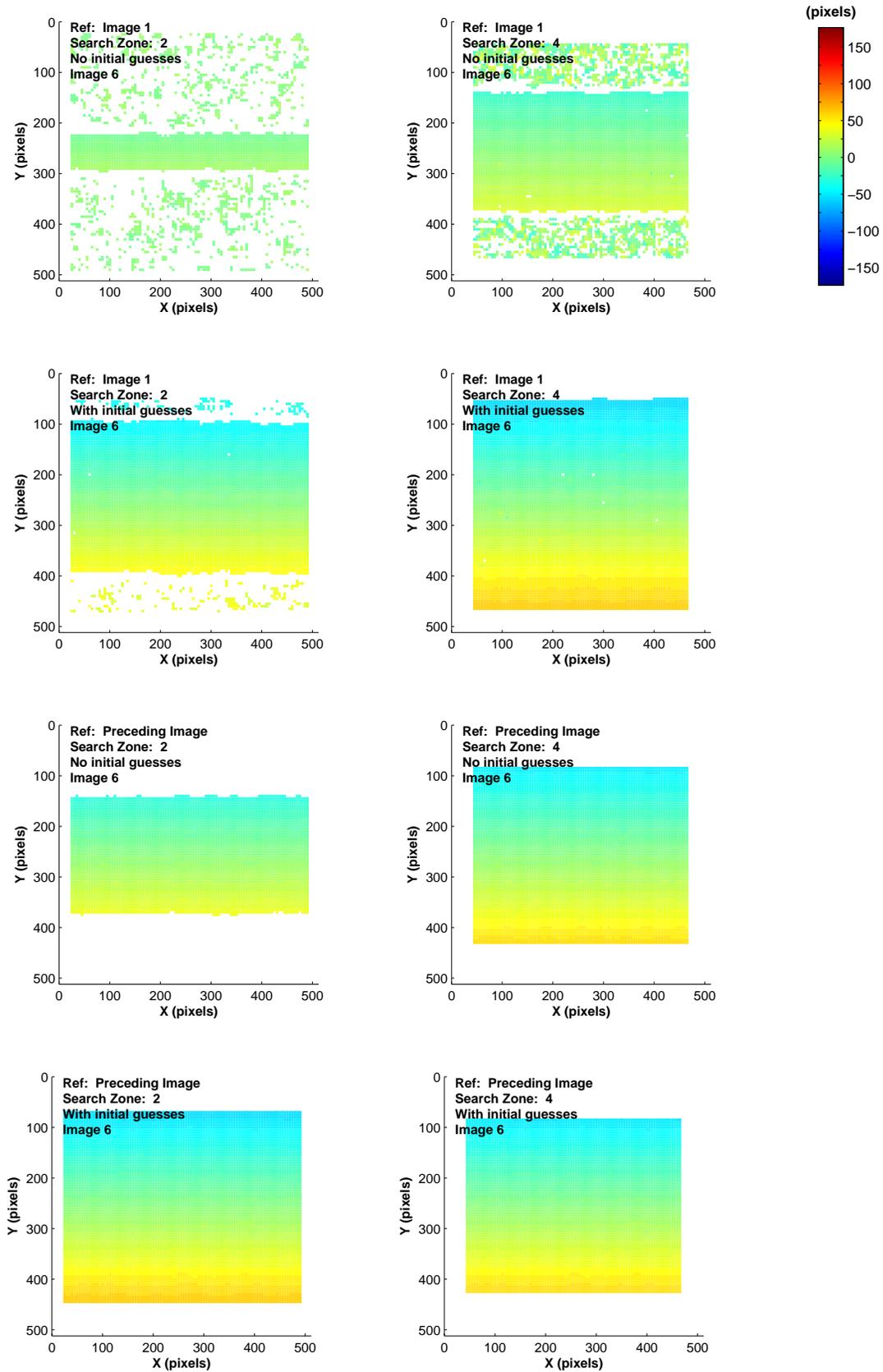
Figure 34: Select contour plots of the vertical displacement, V, for image 6 under different correlation parameters. Initial guesses were obtained by correlating the reduced images using the preceding image as the reference image. For all correlations, a subset of 21 and a threshold of 0.5 were used.
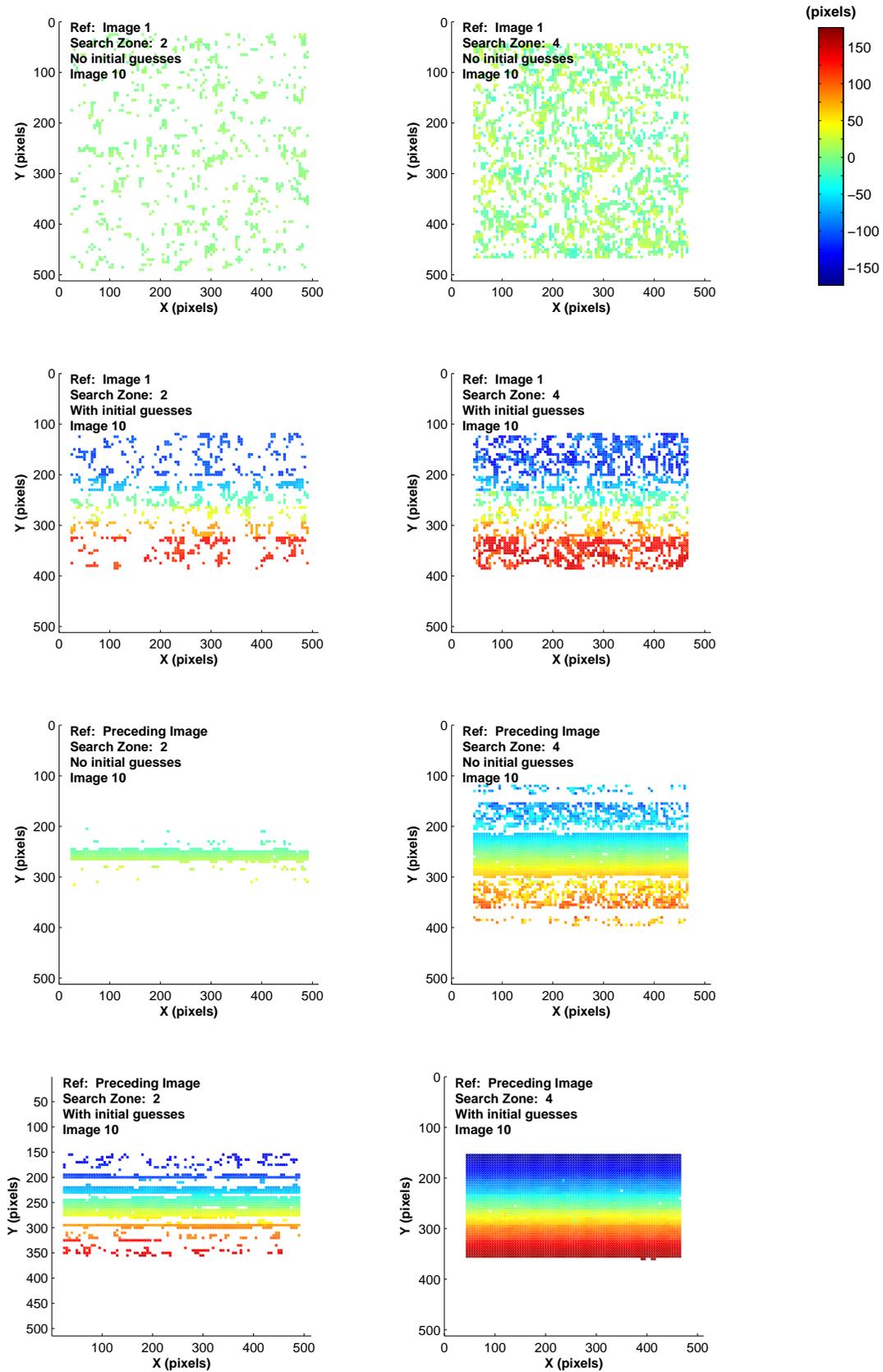
Figure 35: Select contour plots of the vertical displacement, V, for image 10 under different correlation parameters. Initial guesses were obtained by correlating the reduced images using the preceding image as the reference image. For all correlations, a subset of 20 and a threshold of 0.5 were used.
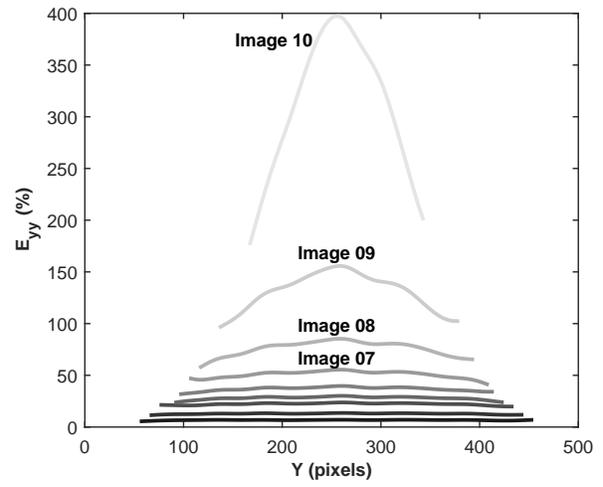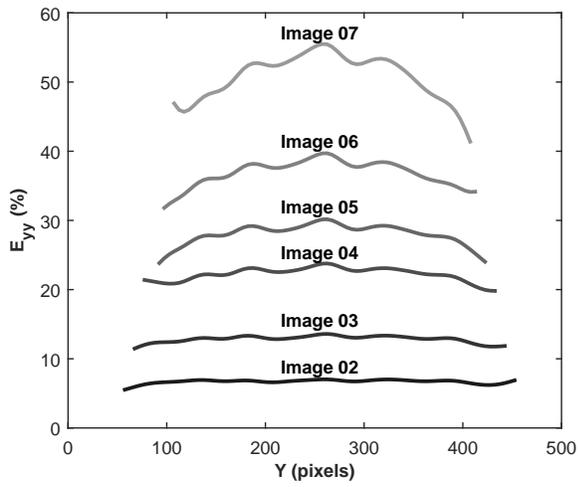
Figure 36: Line scans of the vertical normal strain, E_{yy}, along a vertical line in the center of the image. The smooth kernel size was 11 control points, and three smoothing passes were used.

Sample 11b (Strain Discontinuity)

Deformation: Constant horizontal normal strain on the left (positive strain) and right (negative strain) sides of the image, with a strain discontinuity in the center of the image. Constant strain values for images 2-6: 0.004 %, 0.020 %, 0.039 %, 0.195 % and 0.397 %. the vertical displacements and normal strains are uniformly zero.

Images: 512 x 512 pixels. Same speckle pattern as Sample 09 (rigid rotation).

Results:

The strain values of the constant-strain portions of the first three images (0.004 %, 0.020 %, 0.039 %) are within the noise associated with the strain calculations. Therefore, the ability of the DIC code to capture the strain discontinuity in these images cannot be evaluated. As the displacements are smoothed over the strain discontinuity, the effective width of the discontinuity increases (Fig. 40). These results emphasize the trade-off between obtaining smoother strains in the constant-strain region versus clearly seeing strain discontinuities.


(a)

(b)
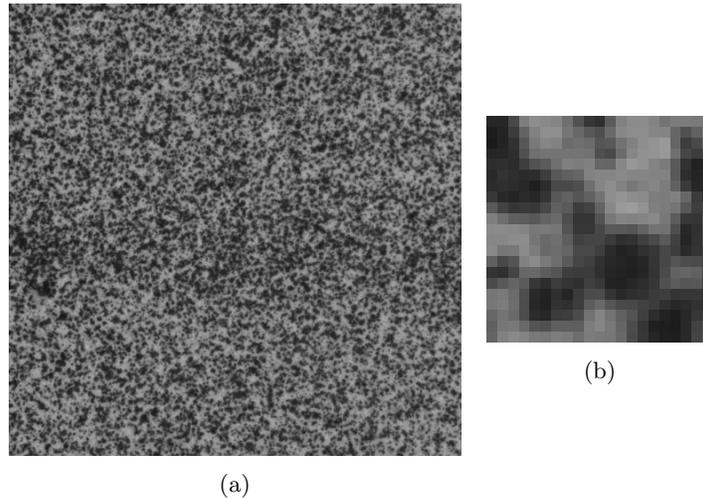
Figure 37: (a) Reference image. (b) Representative subset for subset size 20.
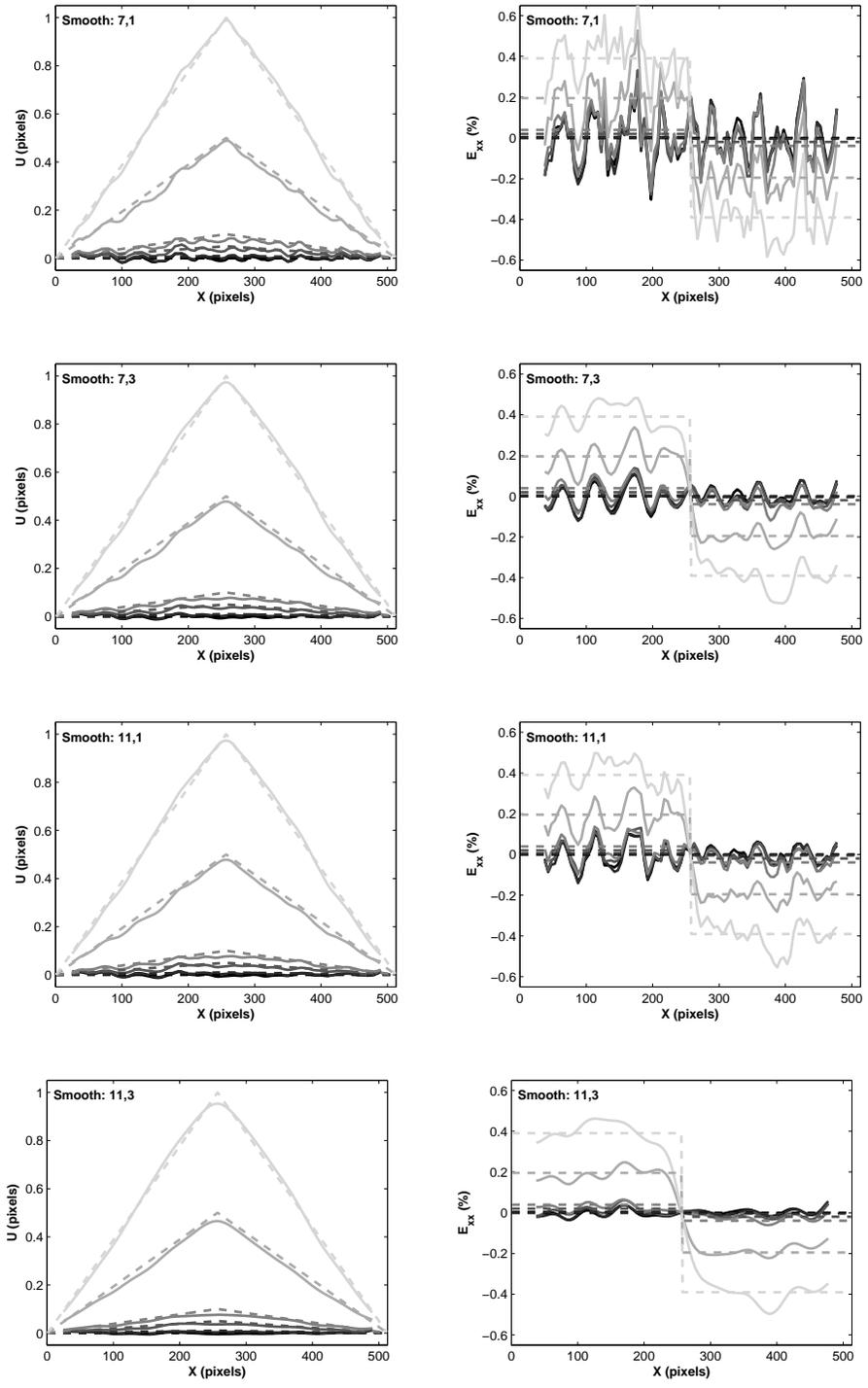
Figure 38: Select line scans of the correlated vertical displacement, V, and vertical normal strain, E_{yy} (solid curves), and the analytic vertical displacement and vertical normal strain (dashed curves) along a vertical line in the center of the image for image 2 (dark curves), image 4 (medium curves), and image 9 (light curves). The subset size for the correlations was 20, and the different smoothing parameters are listed in the figures as [smooth kernel size, number of smoothing passes].
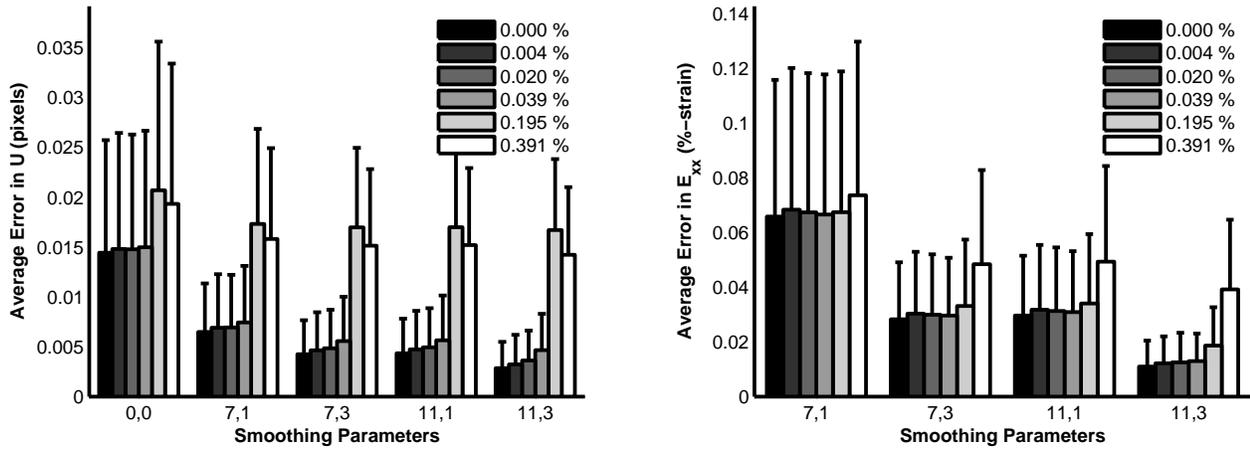
Figure 39: Error, averaged over the left and right regions of the image ($1 \leq x \leq 152$ and $362 \leq x \leq 512$), where the strain is constant, avoiding the strain discontinuity in the center of the image, of horizontal displacement, U, and horizontal normal strain, E_{xx}. The smoothing parameters labeled on the x-axis are [smooth kernel size, number of smoothing passes]. The legend indicates the theoretical value of the strain in the constant-strain portions of the image. The error bars represent one standard deviation.
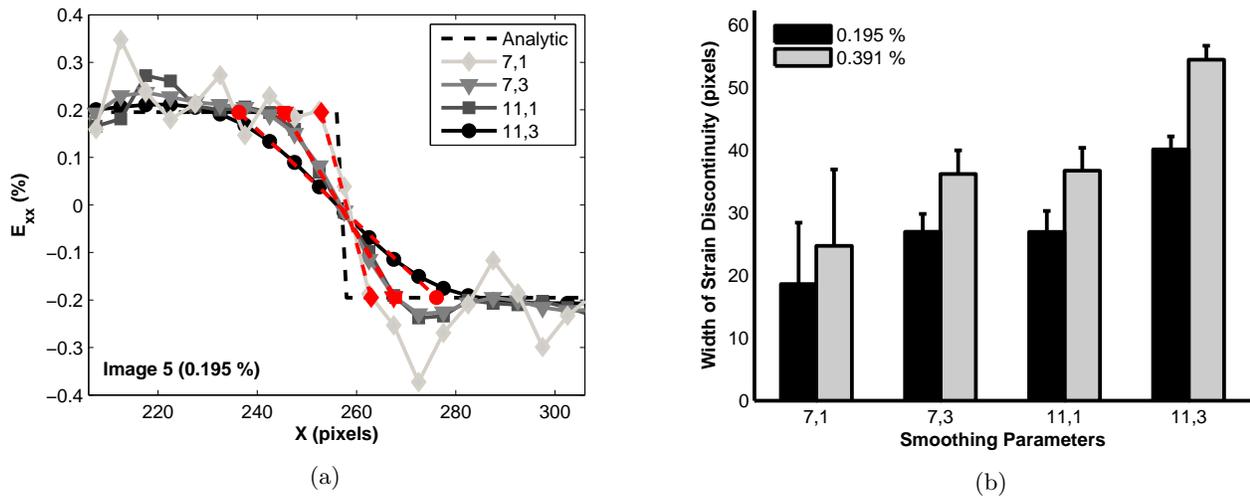

Figure 40: (a) Line scans of image 5 (0.195 % strain) across the center of the image at approximately $y = 256$. The red lines represent the fitting lines used to calculate the width of the strain discontinuity. (b) Average widths of the strain discontinuity for image 5 (0.195 % strain) and image 6 (0.391 % strain). The widths were calculated by fitting a line to the strain data moving across the strain discontinuity. The applied strains for the first four images were smaller than the error in the correlated strains, so the width of the strain discontinuity was not computed for these images. The error bars represent one standard deviation in the calculated widths along the vertical dimension of the images.

Sample 14 (Varying Strain, FFT)

Deformation: Sinusoidal variation in horizontal normal strain with increasing frequency. The vertical displacements are uniformly zero. The horizontal displacements varying only in the horizontal direction and are constant in the vertical direction.

Images: 2048 x 588 pixels. More contrast towards the left side of the image compared to the right side of the image. Speckle pattern constant for all images.

Results:

The spatially-varying strain fields in this image set emphasize the trade-off that occurs when smoothing displacements. One must smooth the displacements sufficiently to have reasonable strain calculations but not so much that the spatial information of the strains is lost. Smoothing with a kernel of 11 grid points and one smoothing pass results in fairly noisy strains. Increasing the number of smoothing passes results in smoother strains but at the expense of computing a lower strain amplitude than the analytic solution, particularly for the higher frequencies of the sinusoidal variation (Fig. 42). Though the amplitude of the strain response suffers in accuracy, the frequency of the strain variation is captured well.

The error in the displacements and strains is fairly constant with increasing frequency of the sinusoidal variations when the displacements are smoothed with a kernel of 11 grid points and 1 smoothing pass (Fig. 43). As the smoothing is increased, the error of the low-frequency variations (i.e. image 2) decreases while the error of the high-frequency variations (i.e. the right portion of image 4) increases. The error averaged over the entire image (Fig. 44) is a competition between less error in the low-frequency regimes and larger area in the high-frequency regimes.


(a)

(b)

(c)
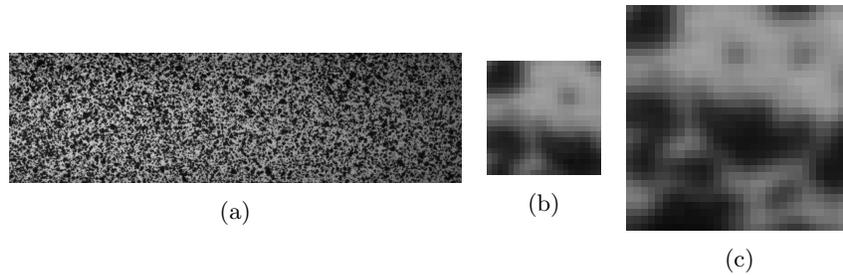
Figure 41: (a) Reference image. (b-c) Representative subsets for subset size 20 and 30 respectively.
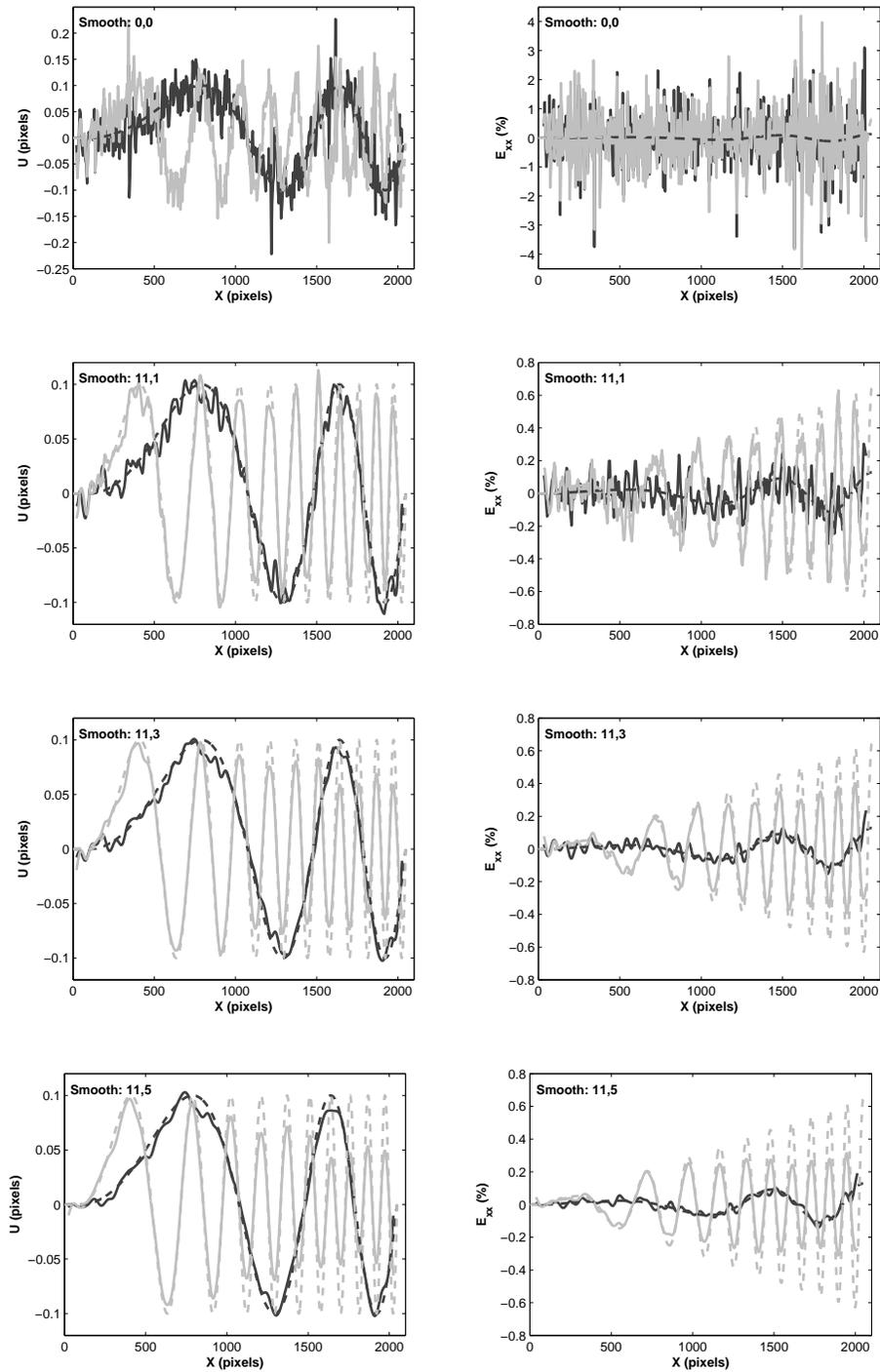
Figure 42: Select line scans of the correlated horizontal displacement, U, and horizontal normal strain, E_{xx} (solid curves), and the analytic horizontal displacement and horizontal normal strain (dashed curves) along a horizontal line in the center of the image for image 2 (dark curves) and image 4 (light curves). The subset size for the correlations was 20, and the different smoothing parameters are listed in the figures as [smooth kernel size, number of smoothing passes].
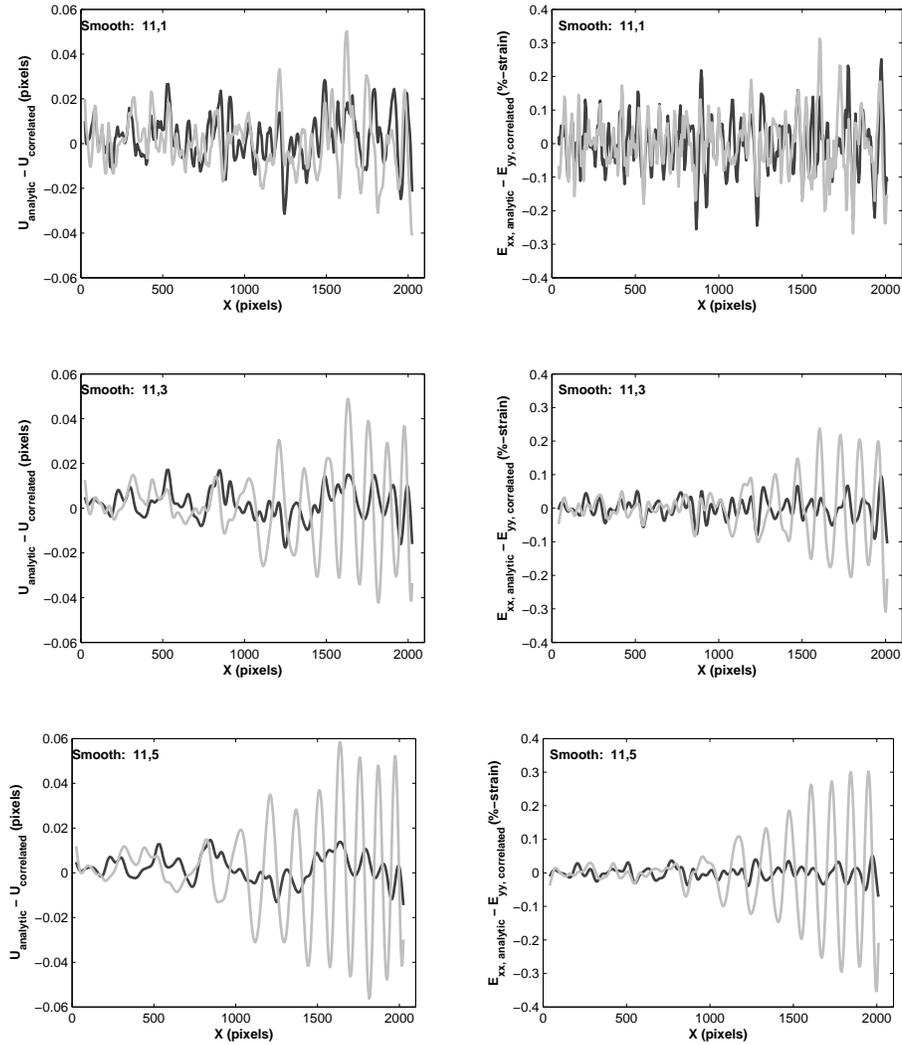
Figure 43: Select line scans of the error of the horizontal displacement, $U_{analytic}$ - $U_{correlated}$, and horizontal normal strain, $E_{xx, analytic}$ - $E_{xx, correlated}$, along a horizontal line in the center of the image for image 2 (dark curves) and image 4 (light curves). The subset size for the correlations was 20, and the different smoothing parameters are listed in the figures as [smooth kernel size, number of smoothing passes].
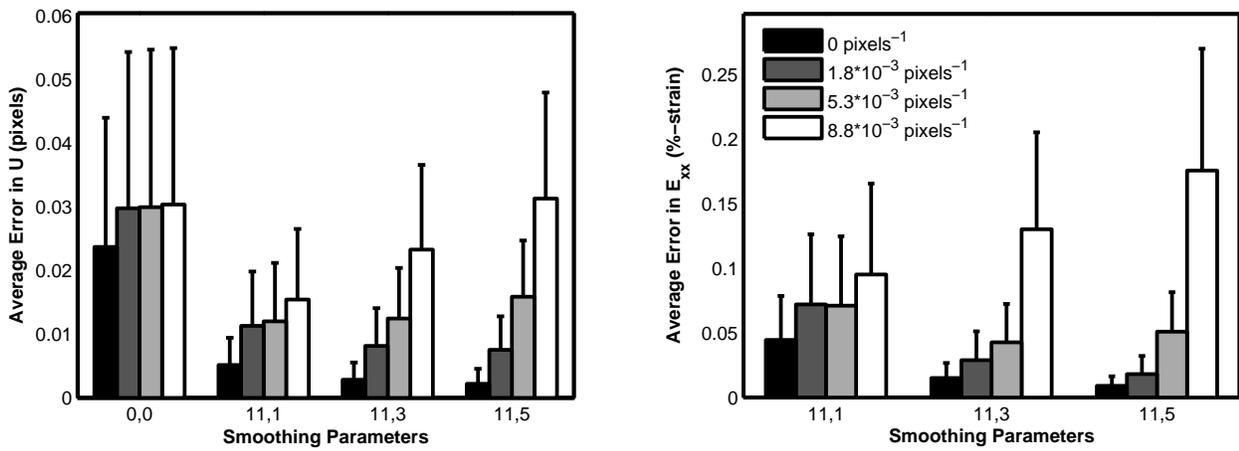
Figure 44: Error, averaged over the right portion of the image where $X \geq 1478$, of the horizontal displacement, U, and horizontal normal strain, E_{xx}. The smoothing parameters labeled on the x-axis are [smooth kernel size, number of smoothing passes]. The legend indicates the average frequency of the applied horizontal normal strain in the right portion of the image where $X \geq 1478$. The error bars represent one standard deviation.

Sample 15 (Varying Strain, TexGen)

Deformation: Modulations of the horizontal normal strain, E_{xx}, with increasing distance between peaks. The horizontal displacements, U, and the horizontal normal strains, E_{xx}, vary only in the horizontal direction and are constant along the vertical direction. The vertical displacements, V, and vertical normal strains, E_{yy}, are uniformly zero.

Images: 2000 x 1000 pixels. Speckle pattern constant for all images.

Results:

The relatively large displacements at the top and bottom of the field of view required the correlation of reduced images to provide initial guesses for the correlation of the full images. The following parameters were used for the reduced image correlation: subset size 20, reduction 3, threshold 0.5.

Similar to the results from Sample 14, the most error is found at the sharpest strain gradients, where the error in the strain can reach 2-3 % strain. Similar to the results from rigid translations, the error in the regions with no strain are approximately 0.03-0.05 % strain. As the ratio of the strain peak spacing to the strain peak width increases, the error of the strain (averaged over the portion of the images with non-zero applied strain) decreases until the ratio is greater than 1 (Fig. **??**). For ratios greater than 1, the error increases slightly, but this is due likely to the full width of the outermost strain peaks falling outside of the image.


(a)　　　　　　　　　　　　　(b)
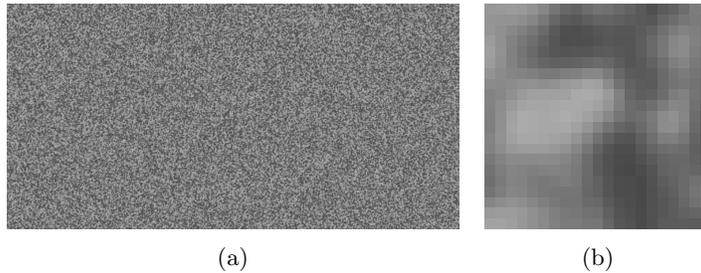
Figure 45: (a) Reference image. (b) Representative subset for subset size 20.
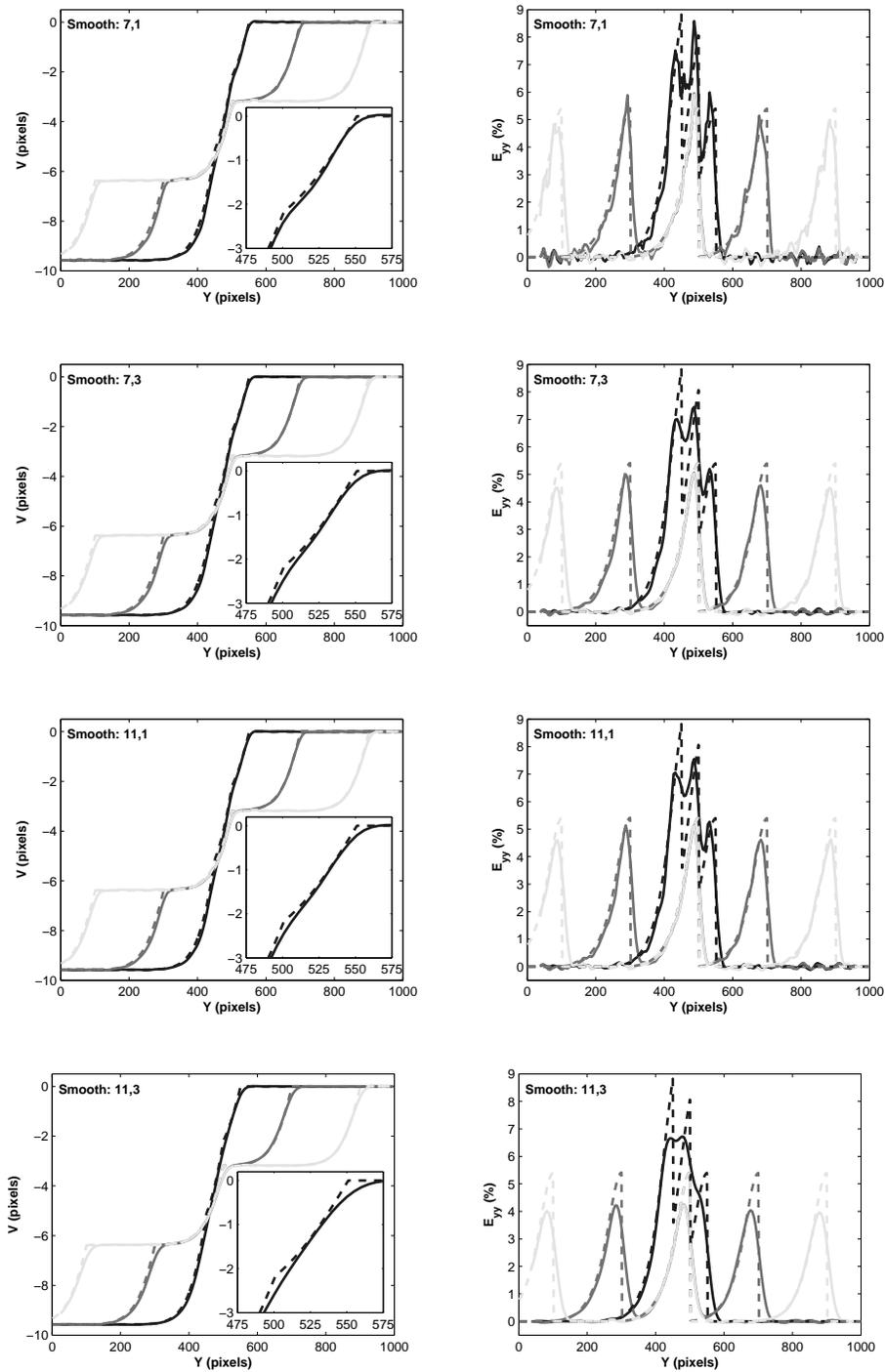
Figure 46: Select line scans of the correlated vertical displacement, V, and vertical normal strain, E_{yy} (solid curves), and the analytic vertical displacement and vertical normal strain (dashed curves) along a vertical line in the center of the image for image 2 (dark curves), image 4 (medium curves), and image 9 (light curves). The subset size for the correlations was 20, and the different smoothing parameters are listed in the figures as [smooth kernel size, number of smoothing passes].
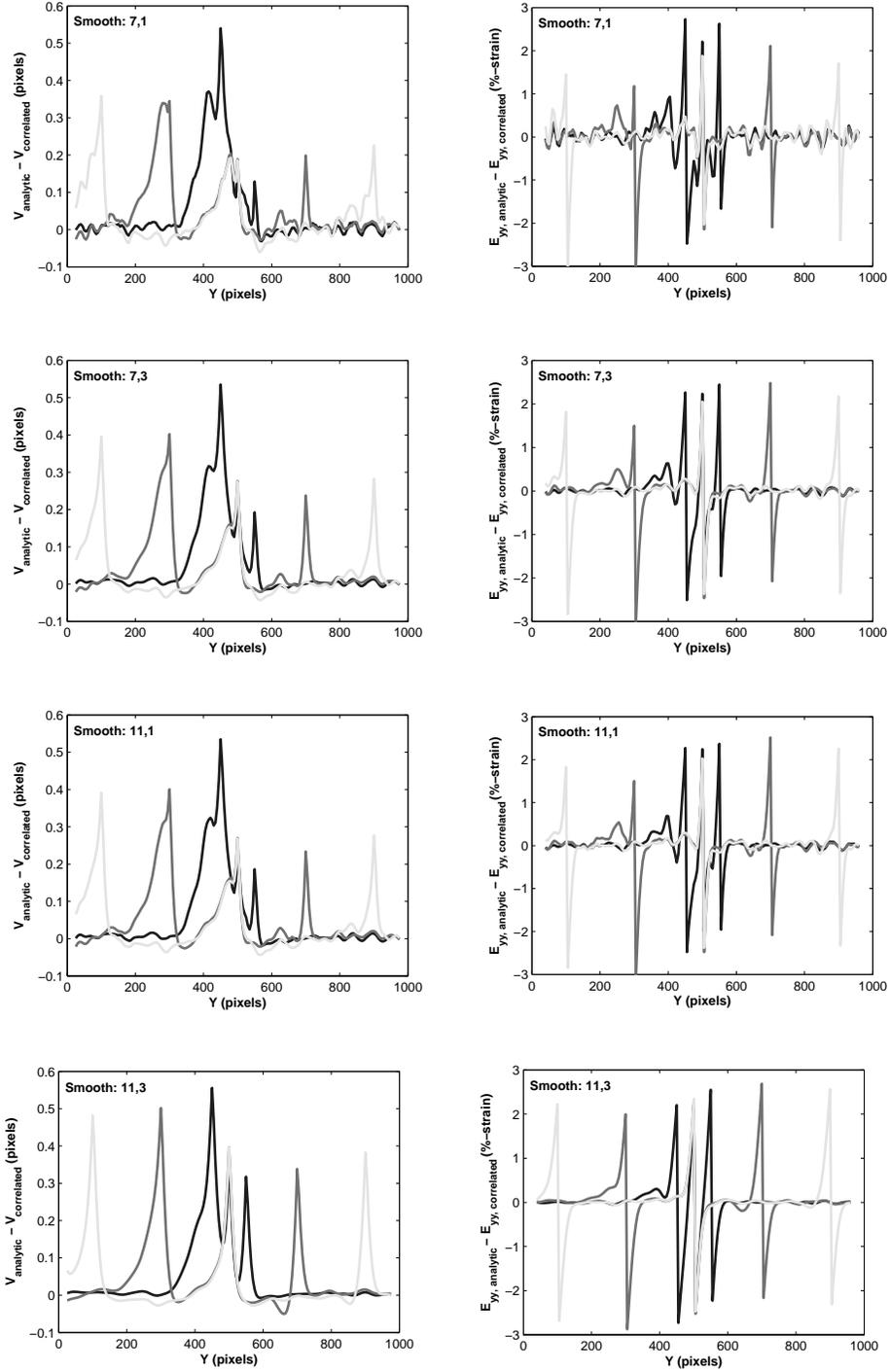
Figure 47: Select line scans of the error of the vertical displacement, $V_{analytic}$ - $V_{correlated}$ and vertical normal strain, $E_{yy, \, analytic}$ - $E_{yy, \, correlated}$, along a vertical line in the center of the image for image 2 (dark curves), image 4 (medium curves), and image 9 (light curves). The subset size for the correlations was 20, and the different smoothing parameters are listed in the figures as [smooth kernel size, number of smoothing passes].
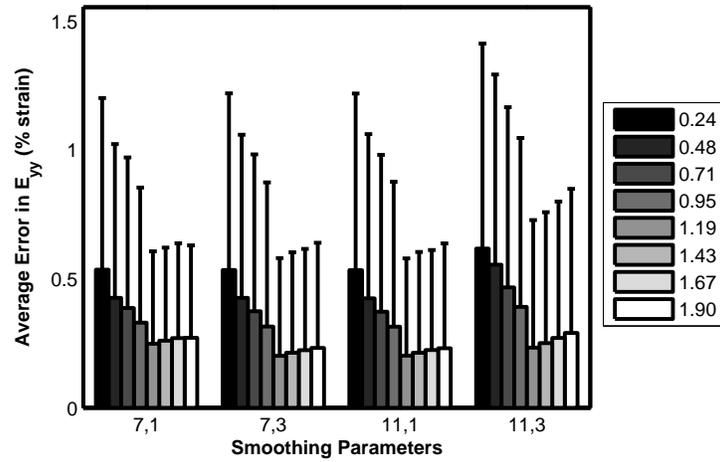
Figure 48: Error, averaged over the portions of the image with non-zero applied vertical normal strain, of the vertical normal strain, E_{yy}. The smoothing parameters labeled on the x-axis are [smooth kernel size, number of smoothing passes]. The legend indicates the ratio of the strain peak spacing (50-450 in 50 pixel increments for images 2-9 respectively) to the strain peak width (estimated as 210 pixels for strains greater than 0.01 %). The error bars represent one standard deviation.